## Campus Placement selection

## CISCO

## Package - 19.14 LPA

# ELECTRA'22

R. C. PATEL
INSTITUTE OF TECHNOLOGY
An Autonomous Institute

## Department of Electrical Engineering

# Vision-Mission

## Institute Vision

To build electrical engineers with a global perspective and a strong dedication to Societal service.

## Institute Mission

To impart high quality Technical Education through :

- Innovative and Interactive learning process and high quality, internationally recognized instructional programs.
- Fostering a scientific temper among students by the means of a liaison with the Academia, Industries and Government.
- Preparing students from diverse backgrounds to have aptitude for research and spirit of Professionalism.
- Inculcating in students a respect for fellow human beings and responsibility towards the society.

## Vision

To build electrical engineers with a global perspective and a strong dedication to Societal service.

## Mission

**M1:** To transform the students from diverse background into skilled electrical engineers.

**M2:** To enhance industrial interaction to meet the changing industrial needs.

**M3:** To serve society with deep awareness of social responsibilities and ethical values.

# HOD's Message

**Dr. Vijay S. Patil**
**Head of Department**

I feel privileged to present our department's “ELECTRA'23” magazine. This magazine is intended to bring out the hidden literary talents among the students and the faculty and teach leadership skills to them.

It will be a source of inspiration for the budding writers among the students. It will direct their creativity to new dimensions of mature expression.

I sincerely thank the editorial team for their constant effort and support in bringing out the magazine in its present form. I thank our Director, Dr J. B. Patil, for their continuous support in preparing these magazine issues.

Lastly, I thank all the authors who have sent their articles.

# CONTENTS

## Section - 1 Technical Article


- Revolutionizing Power Systems: Advancements in Renewable Energy Integration
- Wireless Power Transfer: Beyond Charging Devices
- Battery Advances in Revolutionising Energy Storage
- Next-Generation Solar Panels: Unlocking Efficiency and Durability
- Charging the Future: The Electric Vehicle Revolution
- Renewable Energy Integration: Overcoming Grid Challenges


## Section - 2 Journal Paper


- A Comprehensive Approach to Electricity Billing Management Using Java Swing and SQL
- An Overview of Matlab/Simulink Dynamic Model of an Electric Vehicle's Performance
- Performance and Analysis of Smart Irrigation System Using Internet of Things
- Drone (Quadcopter) for Transmission Line & Solar Panel Cleaning
- Advance Manless E-Vehicle Charging Station
- ARDUINO BASED SMART DUSTBIN
- Smart Energy Meter Using Lora Protocols & IOT Applications
- Development of a Hybrid System Combining Solar and Vertical Axis Power

# SECTION – I

# Technical Article

2021-22

# Revolutionizing Power Systems: Advancements in Renewable Energy Integration

Mr. Yogesh Kirange
Assistant Professor

The global energy landscape is undergoing a dramatic transformation with the rapid integration of renewable energy sources. This issue of the Electrical Engineering Magazine delves into the advancements in renewable energy integration, focusing on the engineering innovations that are revolutionizing power systems.

**1. Smart Grid Technologies: Enabling a Sustainable Future**

- Exploring the role of smart grid technologies in integrating renewable energy sources efficiently.
- Intelligent grid management and control systems for enhanced reliability and stability.

**2. High-Voltage Direct Current (HVDC) Transmission: Powering the Green Revolution**

- Investigating the latest developments in HVDC transmission systems for long-distance renewable energy transmission.
- Overcoming challenges and optimizing efficiency in HVDC systems.

**3. Energy Storage Solutions: Empowering Renewable Energy Reliability**

- Highlighting breakthroughs in energy storage technologies, including batteries, flywheels, and compressed air energy storage.
- Assessing the impact of energy storage on grid stability, load balancing, and peak shaving.

**4. Microgrids: Localized Power Distribution for Resilience and Sustainability**

- Examining the design and operation of microgrids as a means to integrate renewable energy at a local level.
- Case studies showcasing successful microgrid implementations and their benefits.

**5. Power Electronics for Renewable Energy Systems**

- Exploring advancements in power electronics for efficient conversion and control of renewable energy sources.
- Integration of power electronics in wind turbines, solar photovoltaics, and other renewable energy systems.

**6. Electrification of Transportation: Challenges and Opportunities**

- Analyzing the impact of electric vehicles on the electrical grid and charging infrastructure requirements.
- Solutions for managing increased power demand and optimizing charging infrastructure.

**7. Cybersecurity in Power Systems: Protecting Critical Infrastructure**

- Discussing the growing importance of cybersecurity in the context of smart grids and renewable energy integration.
- Strategies for safeguarding power systems against cyber threats and ensuring reliable operation.

**8. Future Trends: The Next Frontier in Renewable Energy Integration**

- Speculating on emerging technologies and future trends that will shape the integration of renewable energy into power systems.
- Potential advancements in energy harvesting, transmission, and distribution.

By exploring these cutting-edge topics, this issue aims to provide electrical engineers, researchers, and industry professionals with valuable insights into the ongoing revolution in power systems and renewable energy integration.

# Wireless Power Transfer: Beyond Charging Devices

Sonawane Prerna
Second Year Electrical Engineering

A revolutionary technique, wireless power transfer has far-reaching applications beyond simple device charging. With this innovative technology, electrical energy can be transferred from a power source to an electronic item without physical connections or cords.

The electromagnetic induction theory serves as the foundation for the idea of wireless power transfer. It entails the creation of a magnetic field by a power source, which a compatible device may effectively absorb and transform back into electrical energy. This technology has created new opportunities for several applications across numerous industries.

Electric vehicles (EVs) are one well-known industry where wireless power transfer has significantly influenced. The need to physically plug electric vehicles into charging stations is removed when charged wirelessly. Due to this convenience, EV owners have more flexibility and freedom, streamlining and simplifying the charging process.

Additionally, wireless power transfer has been extremely useful in the medical field. Traditional battery replacement or recharge procedures for medical implants like pacemakers or insulin pumps were intrusive. These gadgets can now be recharged outside thanks to wireless power transfer, eliminating the need for surgery and improving patient safety and comfort.

Wireless power transfer has uses in industries other than consumer electronics and healthcare. For instance, it makes it possible for sensors, displays, or robotic devices to be powered wirelessly and effectively in factories and manufacturing facilities. Because of the decreased need for unwieldy cords or frequent battery replacements, productivity is boosted, and costs are reduced.

The idea of wireless power transfer has also been expanded to encompass larger-scale systems, such as wireless power grids. These grids could revolutionise how power is distributed and enable energy transfer to remote or inaccessible locations by transmitting electricity over vast distances without requiring extensive infrastructure.

Wireless power transfer does confront several difficulties, despite its many benefits. One such barrier is energy transfer efficiency over greater distances, as energy losses might happen during transmission. Researchers are actively working to advance technology and discover creative solutions to maximise efficiency and reduce power loss.

In conclusion, wireless power transfer has become an innovative technology beyond just charging gadgets. Its uses cut across many industries, providing convenience, adaptability, and efficiency. Wireless power transmission can transform how we power our devices and remodel our energy infrastructure for a more connected and sustainable future as research and development proceed.

# Battery Advances in Revolutionising Energy Storage

Sapkale Harshal
Third Year Electrical Engineering

Energy storage is essential to modern society because it allows us to harness and use electricity effectively. Batteries are one technology at the forefront of advancements in energy storage. Significant developments have been achieved over time, revolutionising the industry and opening up new opportunities. This essay will examine recent battery advancements and emphasise how they have the potential to change the way that energy is produced.

**1. Batteries made of lithium-sulfur:** The creation of lithium-sulfur batteries is one promising innovation. Compared to conventional lithium-ion batteries, these batteries, which use Sulphur as the cathode material, offer a high energy density and a low cost. Recent studies have concentrated on overcoming the drawbacks of lithium-sulphur batteries, such as the solubility of sulphur and the production of undesirable byproducts. These developments may open the door to more effective and affordable energy storage options.

**2. Solid-State Batteries:** Developing solid-state batteries is another important innovation. Solid-state batteries use solid electrolytes instead of the liquid electrolytes used in traditional batteries. Because it reduces the possibility of leaking and increases stability, its design increases safety. Higher energy densities and quicker charging speeds are further benefits of solid-state batteries. These batteries have the potential to revolutionise portable devices and electric vehicles, and researchers are working hard to solve production problems and lengthen the life of these batteries.

**3. Flow Batteries:** Flow batteries have attracted interest as a potential large-scale energy storage solution. Flow batteries, unlike conventional batteries, store energy in external tanks that hold electrolyte solutions. Because of the ability to separate energy storage capacity from power output, flow batteries are very scalable. Flow batteries' energy density and cost-effectiveness have recently been improved, making them a desirable alternative for grid-level energy storage and renewable energy integration.

**4. Sodium-Ion Batteries:** Developed in place of lithium-ion batteries, sodium-ion batteries use abundant sodium resources. Sodium-ion batteries may offer comparable energy storage capabilities for less money. Intending to bring sodium-ion batteries to market soon, researchers actively strive to address their drawbacks, such as lower energy density and shorter cycle life.

Advances in battery technology are revolutionising energy storage, opening up fresh avenues for a reliable and effective energy future. The shift is being driven by improvements in sodium-ion, solid-state, flow, and lithium-sulphur batteries. These innovations not only enhance the efficiency, cost-effectiveness, and performance of energy storage systems but also pave the way for the widespread use of renewable energy sources. We can anticipate a future with clean and dependable energy as experts work to push the limits of battery technology.

# Next-Generation Solar Panels: Unlocking Efficiency and Durability

Patil Aachal
Third Year Electrical Engineering

Solar panels are essential for using solar energy, which has emerged as a viable renewable energy source. The creation of next-generation solar panels has been a focus of study and innovation as technology develops. The solar energy sector will be revolutionised by these cutting-edge solar panels designed to maximise efficiency and longevity. The potential of next-generation solar panels to change the landscape of renewable energy is highlighted in this article as we examine their main characteristics and advantages.

**1. Increased Efficiency:** Next-generation solar panels are engineered to attain much greater energy conversion efficiencies than older models. These panels maximise the capture and conversion of sunlight into practical electricity using cutting-edge materials and manufacturing processes. Modern designs prioritise reducing energy losses via reflection, heat dissipation, and other sources to increase efficiency. Higher energy yields and a quicker return on investment are made possible by improved efficiency, which translates into increased electricity generation and improved system performance for solar power installations.

**2. Advanced Materials:** Next-generation solar panels are built with cutting-edge materials, which boosts their durability and efficiency. For instance, perovskite, a novel semiconductor material, is being investigated for its excellent light absorption capabilities, which could lead to higher conversion efficiencies. Additionally, improvements in surface texturing and anti-reflective coatings help reduce energy loss from reflection and maximise incoming sunshine. These cutting-edge materials significantly improve performance and efficiency for solar panel designs.

**3. Longevity and endurance:** The endurance of next-generation solar panels is ensured by engineering, which also makes them resistant to the effects of the environment. The main emphasis of researchers and producers is the development of sturdy panel designs that can endure harsh temperatures, humidity, and other testing conditions. The panels' operational lifespan is extended by improved encapsulation materials and shielding coatings that protect them from moisture, UV rays, and physical harm. This improved toughness lowers maintenance requirements, boosts the dependability of solar power systems, and results in more consistent energy production throughout the panel's lifetime.

**4. Flexible and Lightweight Designs:** Flexible and lightweight solar panels have attracted much attention recently. The increased design flexibility of these next-generation panels makes them appropriate for various uses, such as curved surfaces, portable gadgets, and wearable technologies. These panels can be effortlessly integrated into many different goods and structures thanks to cutting-edge materials and production processes, increasing the potential solar energy applications. These panels' adaptability and light weight make installation easier and lessen the overall weight strain on structures, creating new opportunities for the use of solar energy.

# Charging the Future: The Electric Vehicle Revolution

Harshal Padmor
Final Year Electrical Engineering

Electric vehicles (EVs) are undergoing a profound transformation that is changing the automotive sector. This revolution is being sparked by the rising desire for more eco-friendly transportation options, a decline in the use of fossil fuels, and the fight against global warming. The vital component of charging infrastructure, which is at the fore of this transformation and is essential to guaranteeing the smooth adoption and broad usage of EVs, is at the forefront. We will discuss The importance of charging infrastructure and its crucial role in determining the future of electric mobility.

**The Importance of Charging Infrastructure:** Electric vehicle (EV) owners can recharge their vehicles thanks to a charging station network. This infrastructure is essential for sustaining the increasing number of EVs on the road today. Convenience, accessibility, and dependability are assured by a vital charging infrastructure, all of which decrease major objections to EV adoption.

**Convenience and Accessibility:** The availability of charging stations is one of the main issues for prospective EV purchasers. A well-designed charging infrastructure offers a network of stations thoughtfully positioned in diverse settings, including homes, businesses, shopping malls, and along main thoroughfares. This ubiquitous accessibility guarantees EV owners the ease of charging their cars whenever necessary, minimising range anxiety and boosting ownership confidence.

**Efficiency and Reliability:** Charging infrastructure is essential to assuring the dependability and effectiveness of EV charging. Modern, fast charging stations with the latest technology make quick recharge periods possible, which minimises downtime for EV owners. Fast-charging stations and other advanced charging infrastructure can provide a significant amount of energy quickly, making long-distance driving possible and equivalent to refuelling at conventional petrol stations.

**Integration with the Power Grid:** Charging infrastructure must be easily linked with the current power grid to allow the broad adoption of EVs. To maximise the usage of renewable energy sources while avoiding overtaxing the grid, this integration necessitates precise planning and coordination. The charging process can be improved, and the load on the power grid during peak times can be reduced with innovative charging technologies like demand response and time-of-use pricing. Additionally, thanks to bidirectional charging technology, EVs can function as mobile energy storage devices, which offers a potential remedy for grid stabilisation and energy management.

**Future Prospects and Challenges**: Infrastructure for electric vehicle charging must keep up with the market's rapid growth. To increase accessibility and convenience for EV owners, governments, businesses, and stakeholders must work together to invest in constructing more charging stations, particularly in public spaces and rural areas. Standardising charging connectors and protocols is essential to ensuring compatibility and interoperability across various EV models and charging stations.

Tushar Patil
Final Year Electrical Engineering

Solar, wind, and hydroelectric power all play key roles in the global energy mix, which is increasingly dominated by renewable energy sources. Renewable energy sources have indisputable environmental advantages, but integrating them into current power systems presents a number of difficulties. In order to ensure a smooth transition to a cleaner and more sustainable energy future, this article examines the grid problems connected with the integration of renewable energy sources and considers potential solutions.

**1. Intermittency and Grid Stability:** Because they are dependent on the weather and natural resources, renewable energy sources are by their very nature intermittent. For example, the intermittent nature of solar and wind energy poses problems for grid stability since jarring changes in generation can put a burden on the infrastructure. Advanced forecasting methods, such machine learning algorithms, can be used to predict renewable energy generation and adjust grid operations as necessary to handle this. Batteries and pumped hydro storage are two examples of energy storage technologies that can be extremely helpful in taming the intermittent character of renewable energy sources, bringing stability, and balancing the supply and demand for electricity.

**2. Grid Infrastructure and Upgrades:** To integrate renewable energy, the grid infrastructure must be upgraded and expanded. New transmission lines must be built since many renewable energy sources are situated in remote locations with poor grid access. Furthermore, to accommodate greater capacity and bi-directional power flows, renewable energy projects energy sometimes necessitate grid modifications. For the development of comprehensive plans for grid expansion and modernization, collaboration between governments, utilities, and private players is essential. This collaboration will help identify locations that need infrastructure expenditures.

**3. consumption Response and Grid Flexibility:** The generation of renewable energy is frequently variable, which may not coincide with conventional consumption patterns. Demand response initiatives and grid flexibility are essential for overcoming this problem. With demand response, customers can modify their electricity usage in response to real-time price or grid operator signals. Renewable energy integration can be optimised by rewarding flexible electricity use, which lowers the demand for traditional backup power sources. Demand response tactics are made possible by smart grid technologies, including automated demand management systems and smart metres.

**4. Regulatory Frameworks and Market Design:** The successful grid integration of renewable energy depends on a supportive regulatory environment. Policies should promote the production of renewable energy, simplify the application procedure for permits, and offer incentives for grid operators to spend money on infrastructure improvements. The full value of renewable energy should also be reflected in market design, which should also include measures to reward flexibility and grid services. Peer-to-peer energy trading and real-time pricing are two examples of cutting-edge market models that can be implemented to make it easier to integrate renewable energy sources and build a more resilient, decentralised grid.

# Journal Papers

DesignEngineering

ISSN: 0011-9342 | Year 2021
Issue: 8 | Pages: 1399-1410

# Data Mining and Machine Learning Based Hybrid Marketing Decision Support System

**Vijay Shrinath Patil[1], Vaishali Bhagwat Patil[2], Jagadish B. Jadhav[3]**

[1]Associate Professor, Electronics &Telecommunications, R C Patel Institute of Technology, Shirpur, vijay. patil@rcpit.ac.in

[2]Professor, Computer Science and Applications, R C Patel Educational Trust's Institute of Management Research and Development, Shirpur, vaishali.imrd@gmail.com

[3]Associate Professor, Electronics &Telecommunications, R C Patel Institute of Technology, Shirpur, jagadish.jadhav@rcpit.ac.in

**Abstract:**

While data mining is often used in engineering and research to address difficulties, finance and marketing also use it to deal with similar issues. With the use of data mining for decision support systems, organizations may better understand their sector and increase their productivity. Because of competition, prices, tax pressures, and other factors, dealing with an unstable economy is the standard for all businesses. A more competitive environment is being created for the business as a result of globalization, localization, and liberalization. In order to achieve targeted benefits and competitive balance, marketing is a difficult job that requires careful preparation and meticulous execution. The marketing decision support system reduces the organization's analysis and strategic planning problems by using an effective data mining technique. An investigation of the above-mentioned organizational marketing methods centered on creating a data mining-based decision support system that included artificial neural networks and decision trees.

**Keywords**: Decision support system(DSS), Data Mining, Artificial Neural Network, Decision Tree.

## 1.Introduction

Computer-based business decisions are becoming increasingly popular, even in small-sized businesses, because of recent technology advancements. According to the study, an organization's

ISSN: 0011-9342 | Year 2021
Issue: 8 | Pages: 1399-1410

market worth improves, therefore benefiting stack holders and owners. These decision support systems have been crafted to reduce the amount of human effort it takes to process data for organizational analysis. This could boost quality in the company in a short period of time by giving timely decisions based on the existing facts. the quality of an organization is defined as Data quality, and decisions about growth can therefore be made when appropriate to direct growth in the proper direction. With decision support systems, data analytics can be used to discover relevant trends, and this, in turn, will allow strategies and solutions to be devised. The decision-making process is heavily reliant on data; thus, a supportive system compiles the relevant information in the form of graphs or text using artificial intelligence. Conventional information such as legacy, assets,and relational data is collected in a decision support system, together with any information relevant to the specific context, and is presented with comparison analysis of future trends. This decision support system is something organizations have started to use on a day-to-day basis.

Frequent collection of sales data with budget and forecast specifics is done to aid in the formulation of a marketing strategy. Information gathering, data analysis, and data reorganization are common approaches used in the development of decision support systems. The diagram shown in Figure 1 displays the overall picture of DSS.

The DSS fall into two basic categories: those that offer active assistance and those that offer passive assistance. The passive approach gathers information and organizes it in an productive manner, but it does not offer any decisions or suggestions that it discovers. It engages in the collection and processing of information to arrive at conclusions and solutions. Meanwhile, the use of human-computer cooperative decision support processes and data collection and analysis permits for additional refinements to the solutions. Decision support system has been divided into different types of applications such as Decision support system driven by

- Data,
- Communication
- Document
- model simulations and
- Knowledge

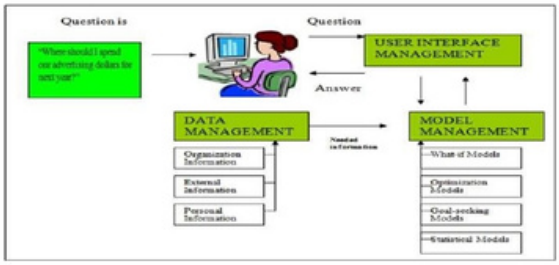


**Fig 1:support system for making decisions**

ISSN: 0011-9342 | Year 2021
Issue: 8 | Pages: 1399-1410

Data-driven decision support (DDDS) systems begin with data collection, as the accumulation of necessary information allows for better decisions to be made in a short period of time. In order to meet the specific user needs, the data needs to be altered, as structured or unstructured data may be obtained from internal and external sources. Time series data manipulation is accomplished by the manipulation of the internal data. In the event that external data is required, it can be obtained through manipulation of the external data. Decision support system that uses data-driven queries will give you a simple file system, which you may access and retrieve using queries. The data-driven strategy is aimed at capturing relevant information on employees, managers, suppliers, and service providers. Communication-driven decision support system analyses allow teams to work together on various tasks even when one member is involved in many processes. Because of this, people collaborate to obtain better strategy, so each member has a different collaborator to help them work together.The communication-driven paradigm concentrates on internal teams and business partners. Communication-centered processes utilizing client-server-based or web-based technologies are extensively adopted as decision-support driven communication processes.

Group-based DSS tools execute operational activities on the basis of a group of users. In document-driven models, finding identifying relevant documents and relevant web is the process. Storing and adaptable technology is vital to document retrieval and analysis in this architecture. Decision in document-driven models is obtained by processing various document types like text documents, spreadsheets and database records. Like communication-based decision support, which also leverages client-server-based technology or web-based, document-driven DSS utilizes that technology to get decisions. To provide highly customized decision support solutions, businesses may choose to modify financial data in order to improve their organizational growth. Since model-driven decision support systems rely on quantitative analysis and offer basic functionality utilizing limited parameters, a small dataset is not required. The goal of a model-driven decision support system is to influence managerial decision making, which is why these systems are frequently implemented as either client-server solutions or stand-alone personal computers.

With knowledge-driven decision support systems, organizations have greater user coverage, including the possibility of interactions with others. A necessary part of a knowledge-driven model is the management council, which makes it possible for a business to determine which service or product is best. It can tell management what to do. The goal of a knowledge-driven strategy is to implement problem-solving solutions that enable easy problem identification. Figure 2 depicts the features and limitations of a decision support system.

DesignEngineering
ISSN: 0011-9342 | Year 2021
Issue: 8 | Pages: 1399-1410

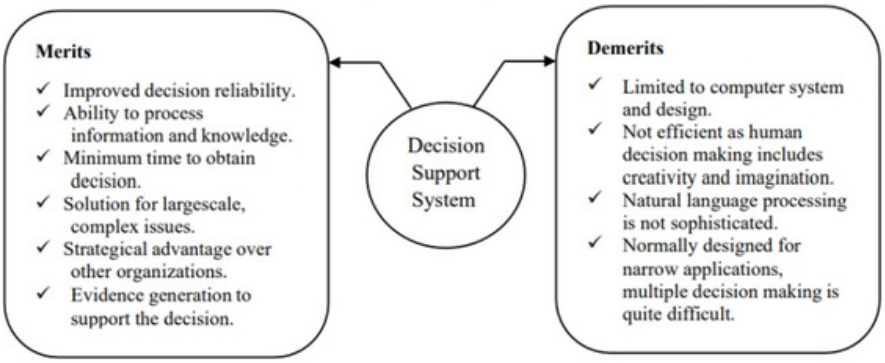


**Fig 2. The Decision Support System Merits and Demerits**

Farmers can utilize decision support systems in agriculture to help them plan crops. According to the analysis, it provides sufficient time for fertilizing, planting, and harvesting for farmers, who can better manage their efforts that way. A decision support system (DSS) is utilized in medical practice to aid in clinical decision making, particularly when it comes to handling complex clinical data. Cost control models, which reduce the repetitious, duplicate medicine purchases and tests, are applied for medical data with diverse types of information such as preventive protocols, tracking orders and protocols. Natural catastrophes such as floods are predicted using decision support systems, which utilize historical weather data as well as real-time meteorological data to come up with predicted events. It allows those sections of the country at risk of flooding to be detected, sparing both financial loss and human casualties. Education institutions use decision support systems to find out specific information on students. Based on the projection, it will be able to predict the number of students who will be on campus next year. Student enrollment is contingent on the outcomes, which means that institutions may plan and organize the student enrollment procedure to attain full strength for running a course.

## 2.Similarly-themed works

Prior knowledge has been gathered about challenges related to decision support systems through a massive research project. The concepts and models that are based on the system design, application domain, and complexity are presented in this part. In a recently published paper (Daniel et al., 2016)[1], a smart maintenance DSS for corporate data was discussed. The study unveiled information the decision-making process and on big data analytics behind the process. In an effort to reduce the cost of the proposed task, a cost reduction method was used. Research delivers higher predicted findings when its analytical decision process is used for case studies. To reduce production system defects, it is important to have knowledge and experience. As shown by the research by Sebastian.et.al. [2], when it comes to obtaining an organizational decision in a distributed production environment, several research considerations must be taken into consideration. Research provides stronger decision support systems for the test and service teams,

ISSN: 0011-9342 | Year 2021
Issue: 8 | Pages: 1399-1410

which is beneficial for the firm as a whole. Gathering fault symptoms as well as test cases and making them accessible to the maintainers enabled them to detect problems. The decision support system proposed by Erozan et al. [3] can help manufacturers manage their production processes. The effort to increase maintenance performance and product reliability is defined by parameters such as utilization duty cycle, rate, stock effects and redundancy. In order to keep key activities, a suggested decision support system is put through a series of tests using industrial datasets, which results in greater reliability.

According to Francesco et al. [4], there are various challenges with group decision support systems. Work with hierarchical process research and it will help you to make noteworthy decisions for the projects at hand. To get the decision, the options are first ranked, then sorted, and finally, the decision maker's preference function is obtained using Bezier curve fitting. The knapsack model utilized, this research utilizes constraints, such as money and class, to guide the selection of options and delivers better results. In short, the group based DSS described in Siddiqui.et.al. [5] was applied to a web-based version. work is done to solve a team problem at a business school. Since the course offerings, stakeholders' assignments, information, observations and timetable preparation are all listed as being multistage issues, the future development of the situation is expected to be ongoing. The proposed workflow model is implemented as a web application that automates the task of creating schedules using an optimization model. The advantages of this decision support system include superior quality and enhanced workflow, which makes conventional spreadsheet-based solutions redundant.

Morteza et al. [6] agreed that financial growth, the delivery status, the number of service attempts, and the stability of the decision-making system were essential aspects of consideration in their decision-making process. Decision making is established through study work in order to get both deployment of quality functions and similarity. The collective decision-making process is aimed at developing agriculture and investment partnerships. The study model developed has a well-rounded decision-making process that improves the overall quality and reliability. An agricultural production system was outlined by researchers Katia et al. that incorporates a decision support system that includes environmental, social, and economic factors. To determine the efficiency, cost, and production parameters, a proposed model uses an evaluation method. The proposed approach uses the semaphore and sustainability index to preserve sustainability.

Research, decision-making on irrigation and the issues it brings are examined in Nicholas et al. [8] In the study endeavor, decision modelling and decision theory are proposed for the identification of tasks in a for real-time decisions and DSS. To turn business challenges into business solutions, online modelling demands the use of ontology of decision and conventional ontology also requires the use of ontology of decision-making. Yang Luo et al. [9] provided the outcomes of this study on the data center and its DSS, which details the temporal availability elements and energy. A four-stage approach was presented to investigate medium-sized commercial data centers' data

ISSN: 0011-9342 | Year 2021
Issue: 8 | Pages: 1399-1410

management challenges. The cost-benefit analysis is favorable given the financial and environmental benefits. The proposed decision-making assistance system aims to provide an optimal thermal recovery approach. The proposed approach will streamline the total use of energy in the data center.

Regular reasoning was demonstrated in Mahsa.et.al. [10] research, which works together to produce a diagnostic with a flawed logic classifier and a triage level determination algorithm. Clinical decision support systems use an emergency service index measure of patient vital signs to produce prediction findings. These vital signs are treated as inputs to fuzzy logic, in which treatment amounts are predicted. Ahmed et al. [11] also argued that a clinical decision support system based on the clustering method is being developed. Leukemic cells are used to make decisions through treatment that determines the characteristics of the inner structure. A study proposition evaluates the work empirically by comparing it with existing decision support systems, which also allow scientists to locate cells of leukemia. Marieke et al. [12] stated that the plasma concentration was assessed by another clinical DSS. A proposed DSS helps to measure plasma concentrations in the examination of patient health.

The problems with rubber production expressed by Muhammad et al. [13] were discovered using a DSS to detect the yields of rubber production in a manufacturing unit with tiny holders of rubber. By integrating the institutional and social dimensions of rubber production, the DSS boosts the viability of management and profitability. The team, led by Zouhair.et.al. [14], developed a proactive DSS to identify vehicle movies susceptible to crashes. Following an examination of the route geometry, driver inputs and current meteorological data, it was found that the machine learning method could best be used to construct the decision support system. Due to the technique provided, the forecast performance is superior to that achieved by data balance solutions.

A knowledge-based decision support system that would help construction companies better understand the various decision criteria involved in prefabricated prefinished volumetric building was proposed by Bon-Gang Hwang et al. In Singapore, to assist in better judgments about the use of prefabricated prefinished volumetric construction, this decision support system was built. By conducting the survey shown above, it can be concluded that the majority of decision support systems rely on statistical models [15]- [18]. The amount of effort involved in using machine learning models is much less than that involved in the implementation of a machine learning model. As a result, the efficiency of the system might be increased. The presented model was built as a hybrid method that incorporates the ability to give accurate decision assistance to the marketing department.

DesignEngineering
ISSN: 0011-9342 | Year 2021
Issue: 8 | Pages: 1399-1410

**3.Proposed work**

In this proposed hybrid model, an artificial neural network model and a decision tree are both combined. This section includes the math required. In a manufacturing company, the Hybrid model is implemented to consider various challenges such as the one they face in their marketing department. A negative image in the environment and shareholders necessitates the use of a decision support system for marketing and production development. There are several forces considered while attempting to appraise the current situation, and this enhances the strategic uses. The list contains a copy is delivered to the team tasked with designing, all the necessary criteria, and managing the project, as well as the marketing team. During this step, responses from the experts and the marketing team are further examined to locate additional sub-criteria required for the proposed system. A new list is developed based on the analysis, and everyone in the team is given the information to collect comments about the criteria that was selected. The last step of the production and marketing process, when the consensus is determined, is done using sub-criteria that are utilized for marketing process and to refine the industry production. Figure 3 depicts the three-phased process flow for the suggested hybrid model, which includes the following: setting a problem, developing a model, and implementing a strategy.

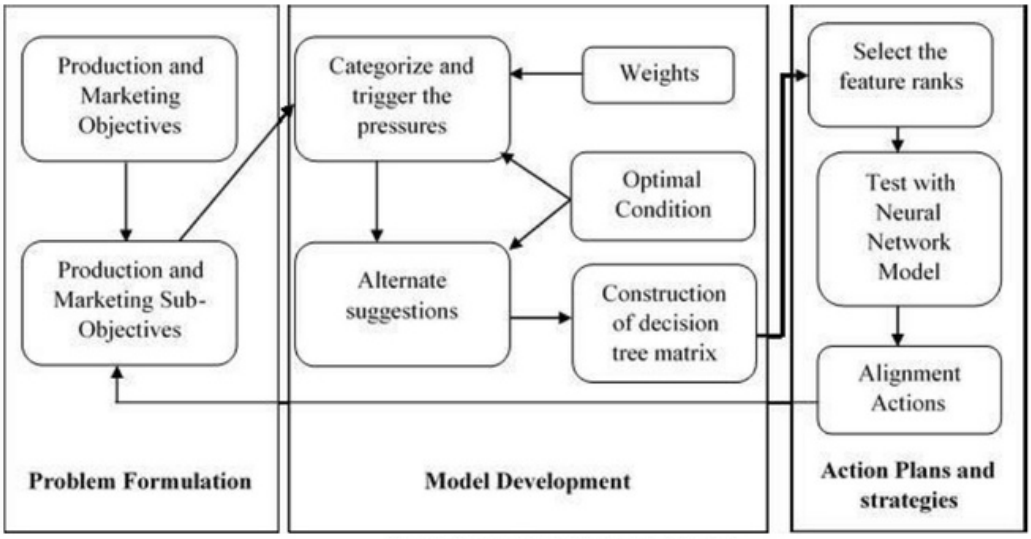


**Fig.3 Proposed Hybrid Model**

The scope and defining the inescapable challenges in the industry are determined during the problem formulation process. This type of analysis is required for DSS in order to establish the main objectives of production and marketing as well as a framework for setting these objectives. Production and marketing objectives are further segmented at the top and bottom levels to better communicate the mission to all personnel. Objective functions, which are based on hierarchical order, are created.

DesignEngineering
ISSN: 0011-9342 | Year 2021
Issue: 8 | Pages: 1399-1410

Formal models are part of the second step of model development. To understand the current production and marketing approach, these models were created based on the sub-objectives. As a matrix function, it is important to consider the constituting, normalizing, and decision tree weight functions.

$$D_{n\times m} = [D_{ij}] \quad (1)$$

An example of how this notion may be implemented in a mathematical formulation is when the column of the matrix represents the various solutions and the line of the matrix is used to represent the pressures triggered. The final matrix function, improved to meet the aim, is $D_{11} \dots \dots D_{1j} \dots \dots D_{1m}$

$$D = \begin{bmatrix} D_{i1} & \cdots D_{ij} \dots & D_{im} \\ \vdots & \ddots & \vdots \\ D_{n1} & \cdots D_{nj} & D_{nm} \end{bmatrix} \quad (2)$$

The Normalized decision matrix is depicted below.

$$D_N = [D'_{ij}]_{n\times m} \quad (3)$$

$where\ D' = \frac{D_{ij}}{i\sqrt{\sqrt{\sum_{k=1}^{n} D'_{kj}}}}, j = 1,2,3 \dots . m.\ i = 1,2,3 \dots . n,$

The artificial neural network is used to refine the outputs of the decision tree model. The model depicted in figure 4 is used to classify the hierarchical decision tree outputs in the DSS.

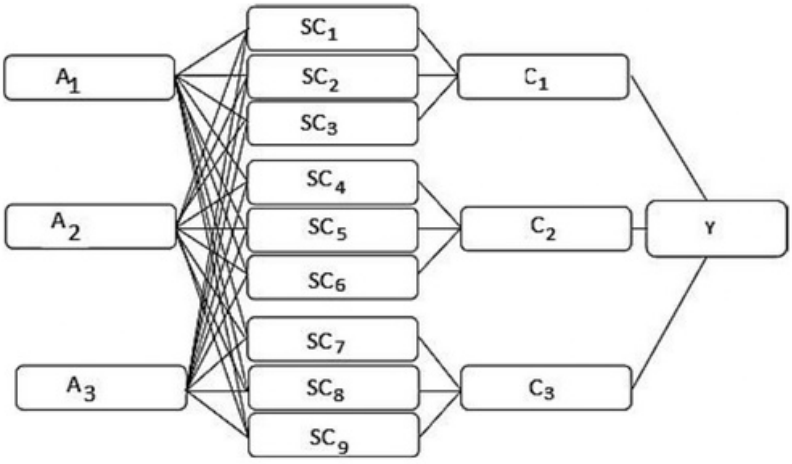


**Fig 4. The neural network model**

ISSN: 0011-9342 | Year 2021
Issue: 8 | Pages: 1399-1410

In order to transform the three level inputs into nine intermediate levels, the transformation process begins at the top-level with the three inputs from the decision tree system, and works its way down into the system's sub-objectives. It shows that the suggested system has top-to-bottom employee contact. The entire purpose of the production and marketing process is cumulated and categorized based on the sub-objective.

**4.Result and Discussion**

Based on the specifications such as parameters, targets ,internal pressure and external forces, the hybrid model presented is analyzed. In order to compare each category to the proposed algorithm and to compare it to other state-of-the-art support vector machine and hidden Markov based decision support systems, all categories must be examined. Objectives for the company, such as profitability, sustainability, and leadership, are stated as A1 for internal pressure, B1 for external pressure, and C1 for company strategy, where subobjectives for the company, such as job satisfaction (SC1), cognitive skills (SC2), employee organization contribution (SC3), employee power (SC4), individual efforts (SC5), response time (SC6 for resources), and company culture (SC7 for company maturity) are listed. The classifications are organized into C1, C2, C3, and then, the resulting decision support system for organizational growth will output its outcomes.

**Table 1. Decision Tree Matrix**

| | $SC_1$ | $SC_2$ | $SC_3$ | $SC_4$ | $SC_5$ | $SC_6$ | $SC_7$ | $SC_8$ | $SC_9$ |
|---|---|---|---|---|---|---|---|---|---|
| $A_1$ | 2 | 2 | 2 | 4 | 4 | 4 | 8 | 5 | 5 |
| $B_1$ | 5 | 5 | 4 | 5 | 5 | 5 | 6 | 3 | 7 |
| $C_1$ | 6 | 8 | 7 | 6 | 5 | 6 | 7 | 8 | 6 |

Table 1 shows how the cluster with respect to the sub-objectives and primary objectives have their decision tree matrix values listed. There are no major differences in the external pressure applied to the three categories. Internal pressure is greater for sub-aims than for overarching objectives. Compared to other employers, our employees put forth significant individual efforts, which is reflected in the traits that signify that our employees are interested in collaborating to improve the organization as an individuals and a team.

Table2 shows the comparison details for the criterion, and it is generated using managers' answers to low-level employees' objectives and sub-objectives. Clustering and threshold values must be consistent for the priority function value to be obtained. If the value is less than 0.1, then it is acceptable, while others are not.

As calculated by multiplying the priority values by the weight associated with each priority value, the proposed system's priority values are compared and measured to the support vector model and hidden Markov model and. This is shown in Figure 5. The suggested approach outperforms other

ISSN: 0011-9342 | Year 2021
Issue: 8 | Pages: 1399-1410

models by evaluating the opinions of the employees, business stakeholders, and management. Due to inefficient assessment procedures, there are less priorities for other models.

**Table 2 Clustering Comparison for the Criteria**

| | | $C_1$ | | | $C_2$ | | | $C_3$ | | | |
|---|---|---|---|---|---|---|---|---|---|---|---|
| | | $SC_1$ | $SC_2$ | $SC_3$ | $SC_4$ | $SC_5$ | $SC_6$ | $SC_7$ | $SC_8$ | $SC_9$ | Priority Function values |
| $C_1$ | $SC_1$ | 1 | 1 | 2 | 3 | 4 | 2 | 4 | 1 | 1 | 0.1671 |
| | $SC_2$ | 1 | 1 | 2 | 3 | 4 | 2 | 3 | 1 | 1 | 0.1671 |
| | $SC_3$ | 1 | 2 | 3 | 1 | 4 | 1 | 2 | 1 | 2 | 0.1467 |
| $C_2$ | $SC_4$ | 1/2 | 1/2 | 1 | 3 | 3 | 2 | 1 | 3 | 3 | 0.0570 |
| | $SC_5$ | 1/3 | 1/2 | 1/3 | 1 | 2 | 2 | 1/4 | 1/4 | 1/2 | 0.0568 |
| | $SC_6$ | 1/4 | 1/4 | 1/3 | 1 | 2 | 2 | 1/2 | 1/2 | 1/4 | 0.0461 |
| $C_3$ | $SC_7$ | 1/3 | 1/3 | 1/3 | 2 | 3 | 3 | 1/4 | 1 | 1/4 | 0.0449 |
| | $SC_8$ | 1/2 | 1/2 | 1 | 4 | 2 | 1 | 1 | 1/4 | 4 | 0.0820 |
| | $SC_9$ | 1/2 | 1 | 1/2 | 4 | 2 | 1 | 1/4 | 1/2 | 1 | 0.1269 |

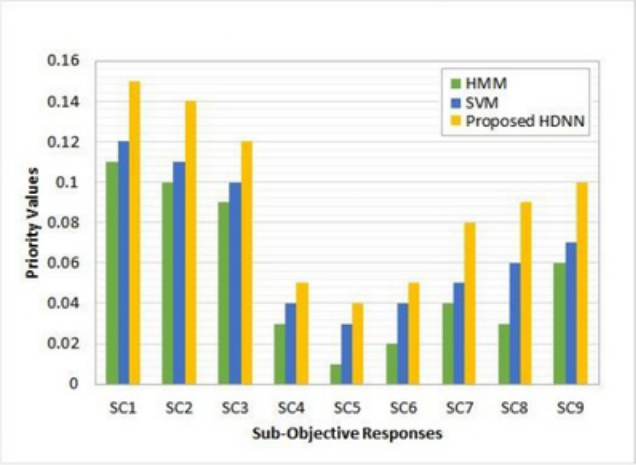


**Fig. 5 Priority assessment comparison**

DesignEngineering

ISSN: 0011-9342 | Year 2021
Issue: 8 | Pages: 1399-1410

## 5. Conclusion

This proposal develops a hybrid decision support system that utilises an artificial neural network and a decision tree. To improve marketing strategies and manufacturing, it is necessary to identify the problems that currently exist in existing decision support models. As a result of employee voting, the main objective function is broken down into many sub-objective functions in order to examine the company from the top to the bottom. Predictions are created by first classifying all the replies, and then an artificial neural network is used to training a decision tree matrix to acquire superior classification strategies. New findings from an experiment are found, compared to support vector machine (SVM) and a traditional hidden Markov Model (HMM) based decision support system, and supported. The presented model outperforms the previous models that may be useful for investigations in various domains. To optimize the assessment, we need to include optimization models in the model.

## References

1. Daniel Bumblauskas, Douglas Gemmill, Amy Igou, Johanna Anzengruber (2017). Smart Maintenance Decision Support Systems (SMDSS) based on corporate big data analytics. Expert Systems with Applications.90: 303-317.
2. Sebastian Abele, Michael Weyrich (2017). Decision Support for Joint Test and Diagnosis of Production Systems based on a Concept of Shared Knowledge. IFAC-PapersOnLine. 50(1): 15227-15232.
3. İhsan Erozan (2019). A fuzzy decision support system for managing maintenance activities of critical components in manufacturing systems. Journal of Manufacturing Systems. 52:110-120.
4. Francesco Lolli, Alessio Ishizaka, Rita Gamberini, Bianca Rimini, Laura Prandini (2017). Requalifying public buildings and utilities using a group decision support system. Journal of Cleaner Production.164: 1081-1092.
5. Atiq W. Siddiqui, Syed Arshad Raza, Zeeshan Muhammad Tariq (2018). A web-based group decision support system for academic term preparation. Decision Support Systems. 114:1-17.
6. Morteza Yazdani, Pascale Zarate, Adama Coulibaly, Edmundas Kazimieras Zavadskas (2017). A group decision making support system in logistics and supply chain management. Expert Systems with Applications.88: 376-392.
7. Katia Regina Evaristo de Jesus, Sérgio Alves Torquato, Pedro Gerber Machado, Catiana Regina Brumatti Zorzo, Dilvan A. Moreira (2019). Sustainability assessment of sugarcane production systems: SustenAgro Decision Support System. Environmental Development. 32:1-15.
8. Nicholas J. Car (2018). USING decision models to enable better irrigation Decision Support Systems. Computers and Electronics in Agriculture.152:290-301.
9. Yang Luo, John Andresen, Henry Clarke, Matthew Rajendra, Mercedes Maroto-Valer (2019). A decision support system for waste heat recovery and energy efficiency improvement in data centres. Applied Energy, 250: 12171224.
10. Mahsa Dehghani Soufi, Taha Samad-Soltani, Samad Shams Vahdati, Peyman Rezaei-Hachesu (2018). Decision support system for triage management: A hybrid approach using rule-based reasoning and fuzzy logic. International Journal of Medical Informatics. 114:35-44.
11. Ahmed S. Negm, Osama A. Hassan, Ahmed H. Kandil (2018). A decision support system for Acute Leukaemia classification based on digital microscopic images. Alexandria Engineering Journal.57(4): 2319-2332.
12. Marieke Pereboom, Inge J. Mulder, Sjoerd L. Verweij, Ruud T. M. van der Hoeven, Matthijs L. Becker (2019). A clinical decision support system to improve adequate dosing of gentamicin and vancomycin. International Journal of Medical Informatics. 124:1-5.

13. Muhammad Fadzli Ali, Ammar Abdul Aziz, Siti Hawa Sulong (2020). The role of decision support systems in smallholder rubber production: Applications, limitations and future directions. Computers and Electronics in Agriculture. 173:1-14.
14. Zouhair Elamrani Abou Elassad, Hajar Mousannif, Hassan Al Moatassime (2020). A proactive decision support system for predicting traffic crash events: A critical analysis of imbalanced class distribution. Knowledge-Based Systems. 205:1-14.
15. Bon-Gang Hwang, Ming Shan, Kit-Ying Looi (2018). Knowledge-based decision support system for prefabricated prefinished volumetric construction. Automation in Construction. 94:168-178.
16. M. Sonika and S. B. G. T. D. Babu, "Analysis of Channel coding performance for wireless communications," J. Study Res., vol. XII, no. 29, pp. 29–49, 2020.
17. C. Srinivasa Rao and S. B. G. Tilak Babu, "Image Authentication Using Local Binary Pattern on the Low Frequency Components," in Lecture Notes in Electrical Engineering, vol. 372, Springer Verlag, 2016, pp. 529–537.
18. S. B. G. T. Babu and C. S. Rao, "Statistical Features based Optimized Technique for Copy Move Forgery Detection," 2020 11th Int. Conf. Comput. Commun. Netw. Technol. ICCCNT 2020, 2020.

# HUMAN GAIT RECOGNITION BY FUZZY REPRESENTATION OF PARTIAL WAVELET COHERENCE



**HUMAN GAIT RECOGNITION BY FUZZY REPRESENTATION OF PARTIAL WAVELET COHERENCE**

**S. A. More[1], V.S. Patil [2], V. B Patil [3], S. A. Patil [4]and A.J. Patil [5]**
GJUS&T,Hisar (India)
[1*, 3, 4] Department of Electronics and Telecommunication Engineering.
R. C. Patel Institute of Technology, Shirpur, India.
[2] Department: Master of Computer Applications, R. C. Patel Educational Trust's, Institute of Management Research and Development, Shirpur, India.
[5]Department of Electronics and Telecommunication Engineering, Samarth Group of Institutions, College of Engineering, Belhe, Tal. Junnar, Dist. Pune, India.
*sagar.more@rcpit.ac.in

## ABSTRACT

*In this paper, a completely unique view invariant gait recognition method based on Partial Wavelet Coherence (PWC) is proposed. We extract 1D signals generated due to movements of hands, legs, shoulders from multi-view gait sequences. The fuzzy representation of the Partial Wavelet Coherence (PWC) of those 1D signals deploy as novel feature for recognition. PWC preserves discriminant information of the individual subject which we use for identification and recognition. The proposed approach has been tested on CASIA multi view database.*

***Keywords***: *Gait recognition, wavelet coherence, cross wavelet transform, partial wavelet coherence.*

## Introduction

Gait recognition has been heavily researched in recent past due to its various advantages like unobtrusiveness, can be captured from distance, work better even with inferiority video and so on. Unlike first generation bio metrics like face, iris, finger print recognition system, this second generation bio metric don't require restricted identification setups and subject cooperation like physical contact with sensor. Gait recognition i.e., identification of people by the way they walk, has gained researchers' attention in last decade and various gait recognition methods are proposed [1], [2], [3], [4].

Gait as bio metric has various challenges. It affects due to some internal or external factors, called as co variate factors. Internal factors are often mood, fatigue, drunkenness, pregnancy (in case of female), injury to foot, change in weight etc. The external factors are often indoor or outdoor environment, surface of walking, wearing shoes or coat, carrying bag, speed of walking etc. Various approaches are proposed for gait recognition. They will be broadly categorized as model free and model based. In model free approach the appearance based image processing techniques are deployed where as in model based approach the physical body dynamics is modeled. Most of the approaches extract features based on shape geometry, pose estimation, modeling physical body then extracting the parameters of model.

The viewing angle plays an important role in gait recognition [5], [6]. The form and dynamics of physical body changes a lot when the sequences captured from different viewing angles of the same person. This is often viewing angle effect. Most of the methods available in literature exploit same viewing angle for training and testing. To show in to view-in-variant and nonrestrictive gait recognition system, the identification method should be unaffected by viewing angle. Even though few approaches like [7], [8], [9] analyze phase variation of the gait cycle for recognition. The coherence based gait recognition approach which is demonstrated during this paper isn't used yet as per our best of knowledge. Next we review some state of the art gait recognition approaches.

## Literature Overview

Model Free Approach: The very initial plan to demonstrate the beholding of motion patterns of human displacement by using moving light display done by Johanson [10]. [1] proposed a way during which they divide silhouette into 7 parts and fit ellipse in those regions. They extract various parameters of

ellipse like; centroid, ratio, major and axis, orientation of axis . All these parameters of seven regions constitute a completely unique feature vector which is then used for person identification. Further [2], [3] use Procrustes shape analysis for automatic gait recognition. First they extract silhouette from the image sequence then apply Procrustes shape analysis method to get mean shape. They use this mean shape as gait signature. Further they employ full Procrustes distance for recognition. Where [3] deploy the static fusion approach during which structural and transitional features extracted and used for recognition. Procrustes analysis used for extracting shape feature and a person's model consists of truncated cone is employed for tracking and recovering joint angle trajectories of lower limb.

A new gait representation has been proposed by [11]. They prepared gait energy image from the sequence of gait images. This representation preserves the temporal information of the sequences during a single averaged image. [12] use fusion of multiple gait cycles for recognition. First they extract silhouette from sequences. The gait cycle is estimated by calculating auto correlation. From each partitioned gait cycle they extract features like gait energy image and motion silhouette image. Finally they use NN classifier.

[13] proposed a 3D method which utilizes complete body shape signature. They extract stereo silhouette vector from 3D contour. They transform this stereo silhouette vector in to 1D stereo gait feature. [14] utilizes the property of radon transform because it guarantees maximum energy for many frequently changing silhouette are like legs and hands alongside various joints. They use Haar wavelet transform first to extract horizontal and vertical features then radon transform applied to construct feature. Hu moment similarity is employed for recognition. Another wavelet based approach [15] uses time - frequency analysis of extracted gait cycle. They calculate area of lower half silhouette image. The gait cycle is made by using the varying area of silhouette image half portion because the subject walk. After wavelet decomposition they calculate mean, variance, skewness and kurtosis of every subject. An easy city block distance measure is employed for identification. [16] proposed a way which is independent of angle of view . First they extract gait cycle which is that the function of width and height of silhouette. Then the temporal matrix is calculated from each gait period. The angle normalization is completed by geometric transformation. LDA is employed for feature analysis. [17] utilizes soft bio metrics like height and stride length during a probabilistic framework for gait recognition. [18] extract spatial and temporal templates which are then projected in to low dimensional space by applying PCA. Canonical analysis is employed for recognition during which accumulated distance is employed as a metric.

**Model based Approach:** In model based approach the human walking mechanism is modeled by some mathematical means. Even though it's has more computational cost it describes physical body dynamics more efficiently. An initial model based attempt for gait-based recognition during a spatio-temporal (XYT) volume is completed by Niyogi and Adelson [4]. First they found the bounding contours of the walker then fit a simplified stick model thereon. A characteristic gait pattern in XYT is generated from the model parameters for recognition. In an- other paper [19] the estimation of hip and knee angles from the body contour by rectilinear regression analysis is given. Then trigonometric polynomial interpolant functions are fitted to the angle sequences and therefore the parameters so obtained are used for recognition. In these model based approaches, the accuracy of human model reconstruction strongly depends on the standard of the extracted human silhouette. Within the presence of noise, the estimated parameters might not be reliable. to get more reliable estimates, Tanawongsuwan and Bobick [20] reconstruct the human structure by tracking 3D sensors attached on fixed joint positions. However, their approach needs many human interaction.

Wang et al. [3] build a 2D human cone model and extract dynamic features from different part for gait recognition. Zhang et al [21] use a simplified five-link biped locomotion human model for gait recognition. Gait features first extracted from image sequences, and then used to train hidden Markov models for recognition. Where in [22] a stick model is developed using HMM with markers placed on body.

In [23] bulk motion, shape and articulated motion estimation was done by gait motion model adaptation. It's a crucial research point within the field of computer vision to recover the coordinate of 3D point from 2D projective images taken by a monocular camera, especially for the camera calibration and 3D reconstruction. In [24] authors have adopted a pair of parallel lines as a feature which is extracted from gait video captured by a monocular camera. It describes the mathematical character of human's walking style. In [25] the 3D model's parameters configuration forms the state vector X and therefore the real image would be the observation Y. Condensation algorithm was used due to its capacity to handle the multi modal and non-Gaussian observation probability. In parallel, they modified the basic algorithm by introducing the interval particle filtering that tends to reconfigure the particles search space in an optimal way. These modifications preserve the benefits of particle filter which offers and have a tendency to scale back the complexity of the essential algorithm. The tactic proposed in one interesting paper [26] considers the fusion of three discriminative component-based features (parameters): 1) the area of each body component 2) the center of each body component, and 3) the orientation of everybody component. The above features are fused supported component and temporal weighting. Experimental results show that the proposed method generally outperforms all other methods that use manual silhouettes.

The angles extracted in defined well frames are utilized for looking for a continuous function, to estimate their successive variation process with reference to time. The function is expanded in Fourier series form in succession, taking under consideration of gait's periodic property. Finally, the vectors composed of Fourier series coefficients are used for classification. In [27] estimation of the position and orientation of the body part, height, stride length, cadence is completed by ellipse fitting and XYT plane slicing. In [28] kinematic gait generative model (KGGM) and the visual gait generative model (VGGM), which represent the kinematics and appearances of a gait are applied to estimate the kinematics of an unknown gait from image sequences taken by one camera. During this paper, we propose a way for gait recognition employing a novel feature supported coherence of various body parts. We use CASIA multi view gait database (Dataset B) consists of 124 persons. Each person is depicted in 10 sequences with various covariate like normal/slow walking, with bag, with coat etc. The sequences are captured at 11 different viewing angles ($0^0$, $18^0$, $36^0$, $54^0$, $72^0$, $90^0$, $108^0$, $126^0$, $144^0$, $162^0$, $180^0$) with reference to frontal view in anticlockwise fashion. Thus the database is contains $124 \times 10 \times 11 = 13,640$ gait sequences. We use binary silhouette provided readily in database for this work. The person is represented by his/her coherence revealed within the body movement during an entire multi period gait cycle at a specific direction. So as to preserve the dynamic body information we utilize partial wavelet coherence which is proposed in geophysics [30]. The similar partial wavelet coherence of varied body poses then extracted by applying k - means clustering to urge Partial Coherent Pose (PCP). The temporal information is preserved by calculating the similarity using fuzzy distance of every test subjects' partial wavelet coherence with all partial coherent poses. For classification the ultimate gait representation i.e. PCP is then projected during a low dimensional discriminant subspace using LDA.

**The main contributions of this work are:**

- The use of partial wavelet coherence as a novel feature for gait recognition.
- The use of partially coherent poses for gait recognition. It is partial wavelet coherence of coordinated body movements at that instant of gait cycle.

## Problem Statement

Let D be the gait database consists of PN

persons, VA viewing angles and CV covariate factors. As mentioned earlier we use CASIA multi view gait database, PN = 124, VA = 11, CV = 10. A view invariant recognition system should identify person walking at any arbitrary angle. Body volume could also be same for various persons at different angle of view. This might be due to view angle effect. The outer appearance of person under investigation could also be suffering from wearing different cloths. Speed of walking is additionally a big covariate factor. In these cases key pose are often observed for a particular gait cycle. It's going to also possible that a specific angle provides significant discrimination of the walking person. For instance gait cycle can't be extracted of an individual walking at an angle $90^0$ to the camera plane i. e. front view.

Gait is that the coordinated movement of physical body, resulted due to leg and hand movements alongside shoulders. The walking style is that the appearance of complete physical body dynamics and co relation among body parts like legs and hands. The foot strike and hand swing are different for various person. During this paper we attempt to explore the co relations among leg swing, hand swing and shoulder swing through partial wavelet coherence.

**Preprocessing**

Each person in CASIA database is walking at VA viewing angles alongside CV covariate factors. Each gait sequence consists of t frames. Because the gait cycle is multi period the number of gait sequences t differs for various sequences. So as to extract various 1D signals we'd like well-defined silhouette. However the silhouettes in CASIA database have many breaks and holes as shown in figure. After labeling the silhouette morphological operations are performed.

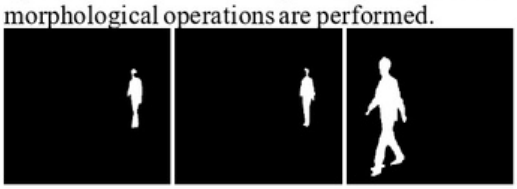

Figure 1: Inferior Images

Further we divide each silhouette in three equal parts which contents different body portion. The primary part contains shoulders. The second part contains hands and third part contains legs. By applying bounding box on each part we extract 1D signal which is variation of width due to movement of shoulders, hands and legs which constitute gait cycle. We extract these three 1D signals form each gait sequence for 7 viewing angles excluding 0°, 18°, 162°, 180°.

Figure 2: A Preprocessed Complete Image

Figure 3: Body parts extracted from a complete silhouette

**Partial Wavelet Coherent Poses (PWCP) Calculation**

Let $X_n$ is 1D signal due to legs movement i.e. gait cycle, $Y_n$ is due to hand swing and $Z_n$ due to shoulder movement extracted from every multi period gait sequence. The partial wavelet coherence is analogous to partial correlation. It reveals coherence between $X_n$ and $Y_n$ after eliminating the persuade of $Z_n$ and following [29] written as,

$$PWC(Xn,Yn,Zn) = \frac{|[WC(Xn,Yn)]-[WC(Xn,Zn)WC(Xn,Yn)^*]|^2}{[1-WC(Xn,Zn)]^2[1-WC(Xn,Yn)]^2} \quad (1)$$

Where, $WC(X_n, Y_n)$ is the wavelet coherence between two time varying signals signals $X_n$ &

$Y_n$ and can be written as,

$$WC(Xn, Yn) = \frac{|S[W(Xn,Yn)]|}{\sqrt{S[W(Xn)] .S[W(Yn)]}} \quad (2)$$

Where, S is smoothing parameter, $[W(X_n)]$ and $[W(Y_n)]$ are wavelet transforms, $[W(X_n; Y_n)]$ is cross wavelet transform of both series. The cross wavelet transform of two given series is given as,

$$W(X_n , Y_n) = W(X_n).W(Y_n)^* \quad (3)$$

Where $W(X_n)$ is continuous wavelet transform and * is complex conjugation.
The cross wavelet power can be defined as,
$W_p = |W(X_n, Y_n)|$ (4)

The local relative phase between Xn and Yn can be expressed as complex argument,

$$\Phi_n = \arg (W(X_n, Y_n)) \quad (5)$$

The complete representation of cross wavelet spectrum is,
$W(X_n, Y_n) = |W(X_n, Y_n)|e^{i\emptyset n}$ (6)

Where $\Phi_n$ is the phase at time tn.

S is the smoothing parameter and expressed as [31]

$$S(W) = S_{scale} (S \text{ time}(W(s))) \quad (7)$$

W $(X_n, Y_n)$ is the cross wavelet transform which exhibits the area of common higher power in the spectrum. Cross wavelet transform of two signals $X_n$ and $Y_n$ is given as,

$$W(X_n, Y_n) = W(X_n).W(Y_n)^* \quad (8)$$

Where W $(X_n)$ is continuous wavelet transform, a zero mean function which already has been proved an efficient tool for time-frequency analysis of non-stationary signals and * is complex conjugation. Being localized in time and frequency, it decomposes the signal at finer resolutions by scaling and translating a mother wavelet function. Following wavelet transform is used as mother wavelet.

$$\psi_0(\eta) = \pi^{\frac{-1}{4}} e^{i\omega_0\eta} e^{\frac{-1}{2}\eta^2} \quad (9)$$

The cross wavelet power can be defined as $|W (X_n, Y_n)|$. The local relative phase between Xn and Yn can be expressed as complex argument arg (W (Xn, Yn)). The complete representation of cross wavelet spectrum is,

$$W (X_n, Y_n) = |W (Xn, Yn)|e^{i\varphi n} \quad (10)$$

Where $\Phi_n$ is the phase at time tn

For each gait sequence we extract mean PWC and finally feature vector is produced $PWC_{mean}^{(PN,VA,CV)}$, $P_N = 1. \ldots, 124$, $V_A = 1 \ldots 7$, $C_V = 1 \ldots 10$.
To produce PWCP, each $PWC_{mean}^{(PN,VA,CV)}$ is used in the training phase. K - means clustering is applied to achieve this. It clusters training $PWC(P_N, V_A, C_V)$ vectors to Q clusters to minimize the within - cluster sum of squares;

$$\sum_{q=1}^{Q} \sum_{i-1}^{PN} \alpha_{iq} \parallel PWC_{mean}^{(PN,VA,CV)} - P_q \parallel^2 \quad (11)$$

where αiq=1 if $PWC_{mean}^{(PN,VA,CV)}$ is assigned to the cluster q and αiq =0 otherwise.
The partial wavelet coherent dynemes $P_q$, q = 1. . . Q are the centers of cluster. It preserve the partial wavelet coherence information of the person captured from a particular viewing angle.

### Fuzzy Representation Of Partial Wavelet Coherent Poses

The $PWC_{mean}^{(PN,VA,CV)}$ vector describes the mean partial wavelet coherence of PNth person, walking at a viewing angle VA and having covariate condition CV. This partial wavelet coherence of each training subject then transformed in to a fuzzy distance. The partial wavelet coherence vectors are mapped to the centroids of the clustered poses$P_q$. The fuzzy distance of each training vector $PWC_{mean}^{(PN,VA,CV)}$ to all $P_q$ are then calculated as follows,

$$q_{fuzzy} = (\parallel PWC_{mean}^{(PN,VA,CV)} - P_q \parallel 2)^{\frac{-2}{m-1}} \quad (12)$$

Where m is the fuzzification parameter and following [23] set to 1.1. Other distances can

also be deployed but fuzzy distance exhibit smooth representation hence preferred. Further for the final representation of the coherence vectors in coherence space, the fuzzy distances normalized to get membership vectors.

$$R_{pwc} = \frac{q_{fuzzy}}{\|q_{fuzzy}\|} \quad (13)$$

To make this cumulative fuzzy membership vector duration invariant as we use multi period gait sequences, the mean of $R_{pwc}$ is taken.
For i = 1,. . ., CV and all tj; j = 1, . . ., pq membership vectors,

$$v_i = \frac{1}{tj} \sum_{k=1}^{tj} R_{pwc}^{ik} \quad (14)$$

**Linear Discriminant Analysis (Lda)**

We apply LDA to $v_i$ to project into low dimensional discriminant subspace in training phase. Each person can be linearly separable in this subspace. In LDA an optimum projection matrix $W_{opt}$ is derived to minimize the fisher criterion.

$$W_{opt} = arg\ min \frac{trace\ W^T S_w W}{trace\ W^T S_b W} \quad (15)$$

Where $S_w$ and $S_b$ are the scatter matrices of within class and between class,

$$Sw = \sum_{n=1}^{C} \sum_{i=1}^{T} \frac{(S_i - \mu_n)(S_i - \mu_n)^T}{N_n} \quad (16)$$

$$Sb = \sum_{n=1}^{C} \frac{(\mu_n - \mu)(\mu_n - \mu)^T}{C} \quad (17)$$

($\mu_n$ is the mean vector of class n and μ is the mean vector of training set. The partial coherent dyanemes membership vector $g_i$ in LDA space then obtained as,

$$g_i = W_{opt}^T v_i \quad (18)$$

In training we use 7 viewing angles. We extract partial wavelet coherence of all the sequences of all the subjects with all the covariate conditions for these angles. In testing we can use all the angles or less. Hence the person can be identified by probabilistic model such as Bayesian framework. Following [23], a priori probabilities can be given as P(PN ), P(VA), P(CV ). Let P(j) is the a priori probability of occurrence of jth person, then a posteriori probability of the j[th] person in the database which get recognized correctly can be given estimated using following formula,

$$(j|P_1, V_1, C_1 \ldots P_N, V_N, C_N) = \frac{P(P_1, V_1, C_1 \ldots P_N, V_N, C_N|j)P(j)}{\sum_{n=1}^{Np} P(P_1, V_1, C_1 \ldots P_N, V_N, C_N|n)P(n)} \quad (19)$$

**Results**

We performed experiments on CASIA gait database B which is described earlier. Figure 4 to Figure 9 shows all the results step by step for a person walking normally at an angle 360. It can be observed that in the initial frames the movements of both legs, hands and shoulder cannot be captured clearly because of self-occlusion. This is due to viewing angle effect. After certain frames, movements of all these body parts can be captured clearly and generate 1D signals as shown in Figure 4 to Figure 6.

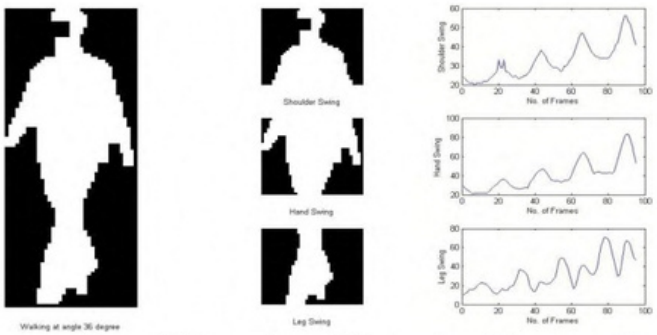


Figure 4: Generation of 1D signals walking normally at $36^0$

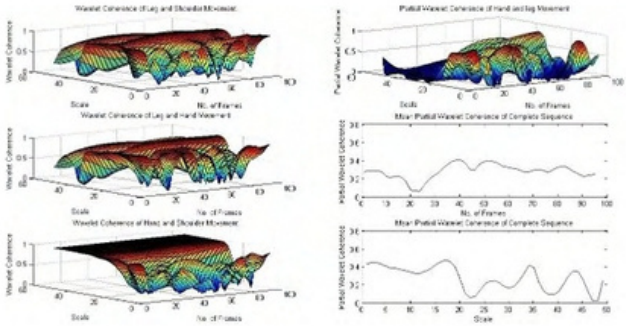

Figure 5: Wavelet Coherence among all 1*D* signals walking normally at $36^0$

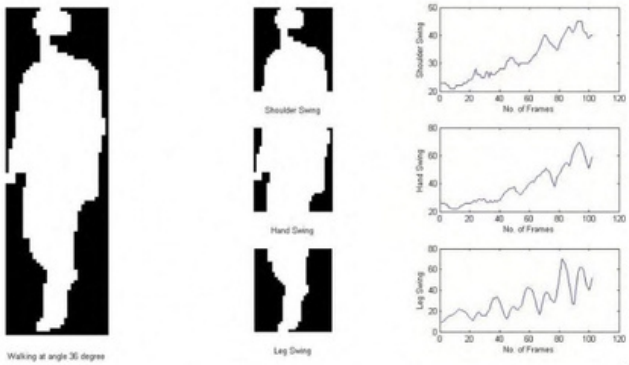

Figure 6: Generation of 1*D* signals walking with bag at $36^0$

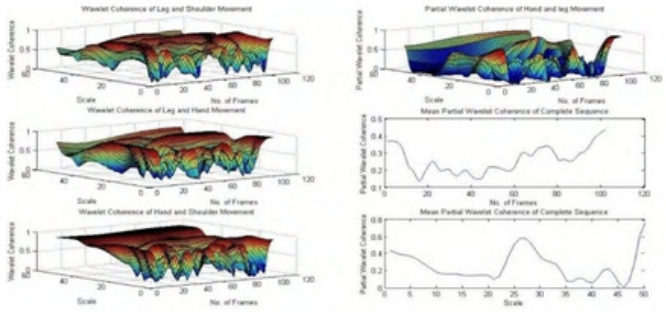

Figure 7: Wavelet Coherence among all 1*D* signals walking with bag at $36^0$

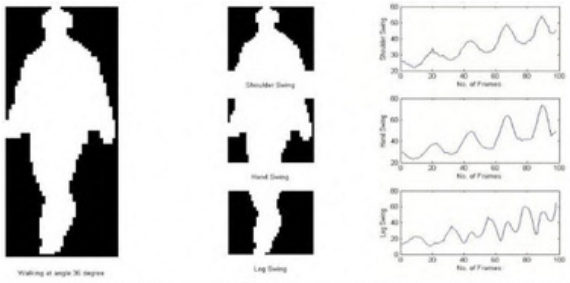

Figure 8: Generation of 1*D* signals walking with coat at $36^0$

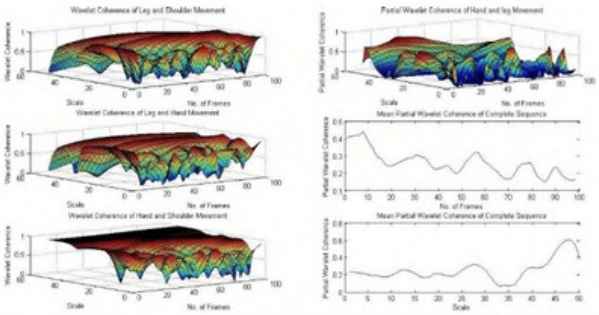

Figure 9: Wavelet Coherence among all 1*D* signals walking with coat at $36^0$

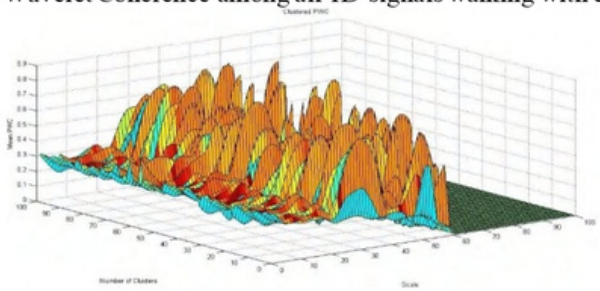

Figure 10: K-means Clustered PWC

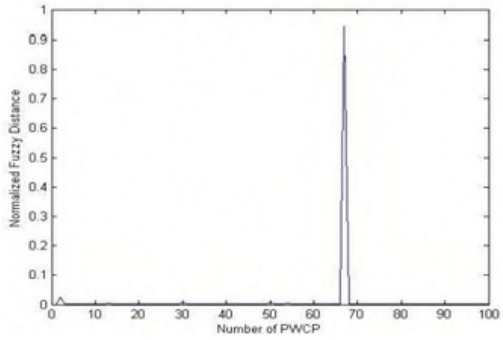


Figure 11: Fuzzy distance of a person walking at angle $36^0$ from PWCP

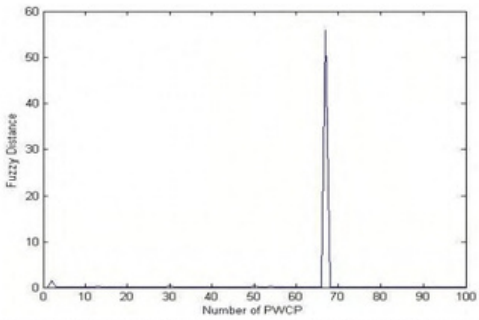


Figure 12: Normalized Fuzzy Membership Vector

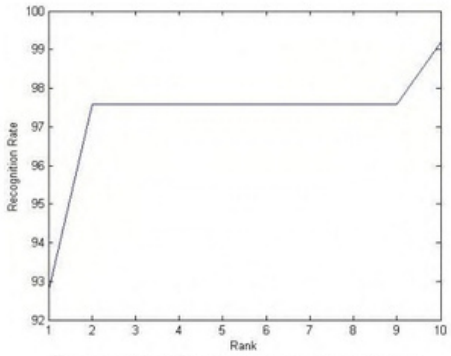


Figure 13: Recognition Accuracy

Table: 1 Comparison

| Method | View-Inv[31] | SEIS [32] | SVM[33] | Proposed |
|---|---|---|---|---|
| Angle/Covariates | 6/10 | 1/10 | 3/10 | 7/10 |
| Recognition Rate | 73.6% | 78.33% | 87.50% | 97.5% |

## Conclusion

In this work we extracted 1D signals from the movement of hands, shoulders and legs of all the gait sequences with all covariate conditions of multi view gait database. Then Partial Wavelet Coherent Poses of those sequences having similar coherence extracted by K-means clustering. The fuzzy distance between partial wavelet coherence of every sequence and clustered partial wavelet coherent poses preserves discriminant information of the walking subject. We got 97.5% mean identification rate. Table 1 shows comparison of proposed method with earlier methods. Even though we got encouraging results the self - occlusion couldn't identified and removed. This might flow from to the binary nature of image. In future we'll attempt to resolve the matter of self – occlusion.

## References

1. L. Lee, W. E. L. Grimson, "Gait analysis for recognition and classification", Proceedings of Fifth IEEE International Conference on Automatic Face Gesture Recognition (Mld), 2002, pp. 734–742.
2. Liang Wang, Tieniu Tan, Weiming Hu, Huazhong Ning, "Automatic gait recognition based on statistical shape analysis", IEEE Transactions on Image Processing, Vol 12, No 9, 2003, pp. 1120–1131.
3. L. Wang, H. Ning, T. Tan, W. Hu, "Fusion of static and dynamic body biometrics for gait recognition", IEEE Transactions on Circuits and Systems for Video Technology, Vol. 14, No. 2, 2004, pp. 149–158.
4. S. A. Niyogi, E. H. Adelson, "Analyzing and Recognizing Walking Figures in XYT", In Proceeding of IEEE Conference on Computer Vision and pattern Recognition, 1994, pp. 469-474
5. S. Yu, D. Tan, T. Tan, Modelling the effect of view angle variation on appearance-based gait recognition, Computer Vision (ACCV 2006), 2006, pp. 807–816.
6. S. Yu, D. Tan, T. Tan, "A framework for evaluating the effect of view angle, clothing and carrying condition on gait recognition", IEEE 18th Int. Conf. Pattern Recognition, 2006, pp. 441–444.

7. I. P. I. Pappas, M. R. Popovic, T. Keller, V. Dietz, M. Morari, "A reliable gait phase detection system", IEEE Transactions on Neural Systems and Rehabilitation Engineering, Vol. 9, No. 2, 2001, pp.113–125.
8. A. Roy, S. Sural, J. Mukherjee, "A hierarchical method combining gait and phase of motion with spatiotemporal model for person re-identification", Pattern Recognition Letters, Vol. 33, No.14, 2012, pp. 1891–1901.
9. J. Wang, C. Lin, "Walking pattern classification and walking distance estimation algorithms using gait phase information", IEEE Transactions on Biomedical Engineering, Vol. 59, No. 10, 2012, pp. 2884–2892.
10. G. Johansson, "Visual perception of biological motion and a model for its analysis", Perception & Psychophysics, Vol. 14, 1973, pp. 210-211.
11. J. Han, B. Bhanu, "Individual recognition using gait energy image", IEEE Transactions on Pattern Analysis and Machine Intelligence, Vol. 28, No. 2, 2006, pp. 316–322.
12. S. H. S. Hong, H. L. H. Lee, E. K. E. Kim, "Fusion of multiple gait cycles for human identification", ICCAS-SICE, 2009, pp. 3171–3175.
13. H. Liu, Y. Cao, Z. Wang, "A novel algorithm of gait recognition", International Conference on Wireless Communications & Signal Processing, 2009, pp. 1–5.
14. H. Z. H. Zhang, Z. L. Z. Liu, "Gait representation and recognition using Haar wavelet and radon transform", WASE International Conference on Information Engineering, 2009, pp. 83–86.
15. Amin T, Hatzinakos, D. "Wavelet analysis of cyclic human gait for recognition", 16th International Conference on Digital Signal Processing, 2009, pp. 1-6.
16. H. Su, G. Y. Chen, "A new method of gait recognition independent of view angle", International Conference on Machine Learning and Cybernet- ics, ICMLC, 2010, pp. 3091–3096.
17. K. Moustakas, D. Tzovaras, G. Stavropoulos, "Gait Recognition Using Geo- metric Features and Soft Biometrics", IEEE Signal Processing Letters, Vol.17, No. 4, 2010, pp. 367–370.
18. P. S. Huang, "Automatic gait recognition via statistical approaches for extended template features", IEEE Transactions on Systems, Man, and Cybernetics, Part B: Cybernetics, Vol. 31, No. 5, 2001, pp. 818–824.
19. J.-H. Y. J.-H. Yoo, M. Nixon, C. Harris, "Model-driven statistical analysis of human gait motion", Proceedings. International Conference on Image Processing, 2002, pp. 285–288.
20. R. Tanawongsuwan, A. Bobick, "Gait recognition from time-normalized joint-angle trajectories in the walking plane", IEEE Computer Society Conference on Computer Vision and Pattern Recognition, 2001. Vol. 2, 2001, pp. II–726–II–731.
21. R. Zhang, C. Vogler, D. Metaxas, "Human gait recognition at sagittal plane" , Image and Vision Computing, Vol. 25, No. 3, 2007, pp. 321–330.
22. S. L. Dockstader, N. S. Imennov, M. J. Berg, a. M. Tekalp, "Fault-tolerant tracking for gait analysis", In Proceedings International Conference on Image Processing, 2003.
23. D. K. Wagg, M. S. Nixon, "On automated model-based extraction and analysis of gait", Proceedings Sixth IEEE International Conference on Automatic Face and Gesture Recognition, 2004, pp. 11–16.
24. Y. Zhang, X. Wu, L. Qi, J. Yang, "A new gait analyzing method under monocular camera", 1st International Conference on Bioinformatics and Biomedical Engineering, ICBBE, 2007, pp. 577–580.
25. J. Saboune, C. Rose, F. Charpillet, "Factored interval particle filtering for gait analysis", Annual International Conference of the IEEE Engineering in Medicine and Biology Society, 2007.
26. N. V. Boulgouris, "Model-based human gait recognition using fusion of features", IEEE International Conference on Acoustics Speech and Signal Processing, 2009, pp. 1469–1472.
27. J. Courtney, a. M. de Paor, "A Monocular Marker-Free Gait Measurement System", IEEE Transactions on Neural Systems and Rehabilitation Engineering, Vol. 18, No.4,

2010, pp. 453–460
28. X. Zhang, G. Fan, "Dual gait generative models for human motion estimation from a single camera", IEEE transactions on systems man and cybernetics Part B, Vol. 40, No. 4, 2010, pp. 1034–1049.
29. E. K. W. Ng, J. C. L. Chan, "Geophysical applications of partial wavelet coherence and multiple wavelet coherence", Journal of Atmospheric and Oceanic Technology, Vol. 29, 2012, pp.1845–1853.
30. A. Grinsted, J. C. Moore, S. Jevrejeva, "Application of the cross wavelet transform and wavelet coherence to geophysical time series", Nonlinear Processes in Geophysics, Vol. 11, No. (5/6), 2004, pp. 561–566.
31. J. N. C. Michela Goffredo, Imed Bouchrika, M. S. Nixon, "Self – calibrating view-invariant gait biometrics", IEEE Transactions on Systems, Man and Cybernetics - Part B: Cybernetics, Vol. 40, No. 4, 2010, pp. 997-1008.
32. N. B. Xiaxy Huang, "Gait recognition with shifted energy image and structural feature extraction", IEEE Transactions on Image Processing, Vol. 21, No. 4, 2012, pp. 2056-2068.
33. D. Ming, C. Zhang, Y. Bai, B. Wan, Y. Hu, K. Luk, "Gait recognition based on multiple views fusion of wavelet descriptor and human skeleton model", IEEE International Conference on Virtual Environments, Human- Computer Interfaces and Measurement Systems (VECIMS), 2009, pp. 246-249

*Vidyabharati International Interdisciplinary Research Journal (Special Issue)* ISSN 2319-4979

# POSE INVARIANT FACE RECOGNITION IN VIDEO

**S.A. Patil*[1], S.A. More [2], V. S. Patil [3], V. B. Patil[4], A. J. Patil[5]**

*[1,2,3]R. C. Patel Institute of Technology, Shirpur, Dist: Dhule, India

[4]Institute of Management Research & Development, Shirpur, Dist: Dhule, India

[5]Samarth Group of Institutions college of Engineering, Belhe, Tal. Junnar, Dist: Pune, India

shailajadp@gmail.com, sagar.more27@gmail.com, vijayshri12@gmail.com, vaishali.imrd@gmail.com, anilj48@gmail.com

## ABSTRACT

*Pose variation is the challenging task in Video-based Face Recognition (VFR) system. The accuracy rate drastically decreases because of pose variation in yaw, pitch and roll angles (Fig. 1). In this paper, we have proposed an approach of Multi-Radius Rotation Invariant Local Binary Pattern (MRRILBP) to VFR for pose variations. We have taken the rotation invariant of three different radius for different sampling points of the same cell, which extracted the detailed features form available face area in pose variation. After pre-processing step the face area is divided into number of blocks, from which Multi-Radius Rotation Invariant Local Binary Pattern (MRRILBP) histograms are extracted. These MRRILBP histograms are high dimensional data features. Independent Component Analysis (ICA) is used to reduce these high dimensional data features. Euclidean Distance (ED) is used for matching the features. We have experimented with different face databases (ORL, NRC- IIT and HONDA-UCSD video database). Experimental results show that our system achieves better performance than other VFR algorithms on pose variation video face databases and thus advancing the state-of-the-art.*

***Keywords**: VFR, MRRILBP, ICA, ED.*

## Introduction

In this paper, our task is to work on pose variation in video face databases. In VFR, we rarely view frontal faces or full face or $0^0$ view. Most commonly, our visual experience of faces falls within a range of viewpoints rotated away from $0^0$ to $45^0$ to the left or right about the vertical axis is called as yaw, above or below about the horizontal axis is called as pitch and clockwise or anticlockwise about the depth axis is called as roll as shown in Fig. 1. We have experimented with three different face databases (ORL, NRC-IIT and HONDA-UCSD), it consist of these three pose variations (yaw, pitch and roll) [1]. Himanshu S. Bhatt, Richa Singh and Mayank Vatsa present a video-based face recognition algorithm that computes a discriminative video signature as an ordered list of still face images from a large dictionary.


Fig.1 Yaw, Pitch and Roll Angle

In his paper [2], as a future research direction, they plan to improve the performance at lower false accept rates. To yield better face recognition performance across large pose variations, from this future scope, we have proposed the MRRILBP to overcome the challenge of large pose variations ($\pm 90^0$). Face recognition algorithms are distinguished between model based and appearance based algorithms [3], [4], [5], model based algorithms use 2D or 3D face models and appearance based algorithms directly use image pixels or features extracted from image pixels. The literature survey shows that many efforts have been taken into the pose

invariant face recognition. David J. Baymer described the earliest appearance-based multi-view algorithm [6]. The algorithm geometrically aligns the probe images to candidate poses of the gallery subjects using the automatically determined locations of three feature points. Pentland et. al proposed a view-based approach to localize the object (or features on an object) and identify the correct 2D aspect [7]. M. Turk and Alex Pentland extended eigenface approach for face recognition [8]. Xi Yin and Xiaoming Liu proposed CNN-based MTL works of an energy-based weight analysis method [9]. Manar D. Samad and Khan M. Iftekharuddin proposed a novel Frenet frame-based generalized space curve representation method for 3D pose invariant face and facial expression recognition and classification [10]. Changxing Ding et. al proposed a novel face identification framework capable of handling the full range of pose variations within $90^0$ of yaw [11]. Poonam Sharma et. al proposed a novel pose invariant face recognition method by combining curvelet invariant moments with curvelet neural network [12]. Sihao Ding et. al [13] presents a novel VFR algorithm using a sequential sampling and updating scheme, named sequential sample consensus (SSC). The proposed algorithm aims at providing a sequential scheme that can be applied to streaming video data. Ding proposed one limitation of the algorithm (SSC) is the requirement of a training video sequence of the frontal views of faces; it is difficult to recognize if the large poses appearing in the training videos are mostly different from those in the testing videos [13]. Kavita Singh et. al [14] presents a pose invariant face recognition system to annihilate pose problem by using a modified log Gabor algorithm and the concepts of rough sets together. In this paper, she present that most of the face images have shown pretty good results at full frontal faces and $\pm 20^0$ offset, but as soon as one goes towards the larger degree of orientations, there have been problems. Algorithm which is designed to work best with pose variation faces images. In many applications, it is not possible to meet these conditions. Some examples are surveillance, automatic tagging, and human robot interaction. Therefore, there have been many recent efforts to develop algorithms that perform well with unconstrained face images. From the above literature survey, we found that many researchers worked on pose variation challenge on face image databases. Pose variation in video-based face recognition is still unsolved problem. In video face database the person can move his/her face in any angle, as this is a natural human tendency while talking. In this paper, we address the pose variation problem to

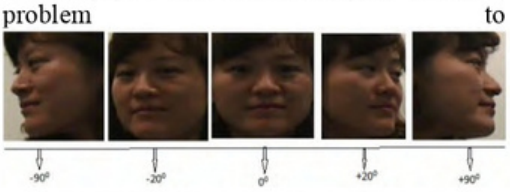


Fig.2 Pose Variation from $0^0$ to $90^0$

combination of Multi-Radius Rotation Invariant Local Binary Pattern (MRRILBP), Independent Component Analysis (ICA) and Euclidean Distance (ED). The novelty of our system is that, it recognises the face in $0^0$ to $90^0$ angle in left and right profile (Fig. 2) from video face database. The database consists of male/female videos, moving their face in any angle. In one video it consists of 14 frames/second, nearby 300 frames in each Video. Video is a combination of frames/images with respect to time. The generic local binary pattern operator is derived from this joint distribution. As in the case of basic LBP, it is obtained by summing the threshold differences weighted by powers of two. The LBPP; R operator is defined as

$$LBP_{P,R}(x_c, y_c) = \sum_{p=0}^{P-1} s(g_p - g_c) 2^p \qquad (1)$$

rotations of a textured input image cause the LBP patterns to translate into a different location and to rotate about their origin. Computing the histogram of LBP codes normalizes for translation, and normalization for rotation is achieved by rotation invariant mapping. In this mapping, each LBP binary code is circularly rotated into its minimum value i

$$LBP^{ri}_{P,R} = \min ROR(LBP_{P,R} i) \qquad (2)$$

where ROR(x; i) denotes the circular bitwise right rotation of bit sequence x by i steps. Omitting sampling artifacts, the histogram of $LBP^{ri}_{P,R}$ codes is invariant only to rotations of

input image by angles $a\frac{360^0}{P}$ $a=0,1,...,P-1$.

However classification experiments show that this descriptor is very robust to in-plane rotations of images by any angle.

The rotation invariant LBP descriptor discussed above defined a mapping for individual LBP codes so that the histogram of the mapped codes is rotation invariant. In this section, a family of histogram transformations is presented that can be used to compute rotation invariant features from a uniform LBP histogram. Consider the uniform LBP histograms $h_I(UP(n,r))$. The histogram value $h_I$ at bin $U_P(n,r)$ is the number of occurrences of uniform pattern $U_P(n,r)$ in image I. If the image I is rotated by $\alpha = a\frac{360^0}{P}$ this rotation of the input image causes a cyclic shift in the histogram along each of the rows,

$$h_{I\alpha^0}(U_P(n,r+a)) = h_I(U_P(n,r)) \quad (3)$$

To achieve invariance to rotations of input image, features computed along the input histogram rows and are invariant to cyclic shifts can be used. Discrete Fourier Transform is used to construct these features.

Let $H_{(n)}$ be the DFT of $n^{th}$ row of the histogram $h_I(U_P(n,r))$ i.e.

$$H(n,u) = \sum_{r=0}^{P-1} h_I(U_P(n,r)) e^{-i2\pi ur/P} \quad (4)$$

In [15] was shown that the Fourier magnitude spectrum

$$|H(n,u)| = \sqrt{H(n,u)\overline{H(n,u)}} \quad (5)$$

of the histogram rows results in features that are invariant to rotations of the input image.Based on this property, LBP-HF feature vector consisting of

three LBP histogram values (all zeros, all ones, non-uniform) and Fourier magnitude spectrum values was defined. The feature vectors have the following form:

$$f^v_{LBP-HF} = \left[ |H(1,0)|,...,\left|H\left(1,\frac{P}{2}\right)\right|, \right.$$

$$|H(P-1,0)|,...,|H(P-1,P/2)|,$$

$$h(U_P(0,0)), h(U_P(P,0)),$$

$$\left. h(U_P(P+1,0))_{((P-1)(P/2+1)+3)} \right]$$

It should also be noted that the Fourier magnitude spectrum contains rotation invariant uniform pattern features $LBP^{riu2}$ as a subset, since

$$|H(n,0)| = \sum h_I(U_P(n,r)) = hLBP^{riu2(n)} \quad (6)$$

An illustration of these features are as shown in Fig. 3.

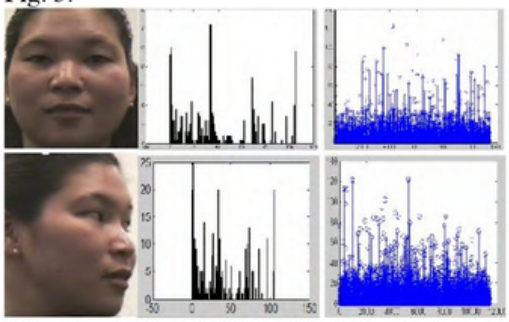

Fig. 3. 1st column: Original Frame at Orientations $0^0$ (Training Frame) and $90^0$ (Testing Frame). 2nd column: bins 1-256 of the Corresponding $LBP^{ri2}$ Histograms. 3rd column: Rotation Invariant Features $|H(n,u)|, 1 \le n \le 7$, $LBP^{ri2}$.

**Independent Component Analysis (ICA)**

The performance of ICA depends on the features extracted by Multi-radius Rotation Invariant Local Binary Pattern (MRRILBP). ICA can be applied so as to treat MRRILBP features as random variables. This paper explores this space, in order to find the best technique for recognizing faces in pose variation video databases. The basis vectors that define any subspace can be thought of as image features. ICA architecture produce global features, in the sense that every image feature is influenced by every pixel. It makes them either susceptible to pose variations or sensitive to holistic properties. This paper shows that the algorithm depends first and foremost on the nature of the task. One characteristic of both PCA and PCA and LDA is that they produce spatially global feature

vectors. In other words, the basis vectors produced by PCA and LDA are non-zero for almost all dimensions, implying that a change to a single input pixel is altering every dimension of its subspace projection. There is also a lot of interest in techniques that create spatially localized feature vectors, in the hopes that they might be less susceptible to occlusion and would implement recognition by parts. The most common method for generating spatially localized features is to apply independent component analysis (ICA) to produce basis vectors that are statistically independent (not just linearly decorrelated, as with PCA). Non-negative matrix factorization (NMF) is another method for generating localized feature vectors. ICA can also be used to create feature vectors that uniformly distribute data samples in subspace. This conceptually very different use of ICA produces feature vectors that are not spatially localized. Instead, it produces feature vectors that draw fine distinctions between similar images in order to spread the samples in subspace. Keeping with the terminology introduced, we refer to the use of ICA to produce statistically independent compressed LDA is that they produce spatially global feature vectors. In other words, the basis vectors produced by PCA and LDA are non-zero for almost all dimensions, implying that a change to a single input pixel is altering every dimension of its subspace projection. There is also a lot of interest in techniques that create spatially localized feature vectors, in the hopes that they might be less susceptible to occlusion and would implement recognition by parts. The most common method for generating spatially localized features is to apply independent component analysis (ICA) to produce basis vectors that are statistically independent (not just linearly decorrelated, as with PCA). images. It generates compressed data with minimum mean squared reprojection error, ICA minimizes both second-order and higher-order dependencies in the input. It is intimately related to the blind source separation (BSS) problem, where the goal is to decompose an observed signal into a linear combination of unknown independent signals. Let $s$ be the vector of unknown source signals and $x$ be the vector of observed mixtures. If A is the unknown mixing matrix, then the mixing model is written as:

$$x = As \qquad (7)$$

It is assumed that the source signals are independent of each other and the mixing matrix $A$ is invertible. Based on these assumptions and the observed mixtures, ICA algorithms try to find the mixing matrix A or the separating matrix $W$ such that:

$$u = Wx = WAs \qquad (8)$$

The equation 8 is an estimation of the independent source signals (Fig. 4)

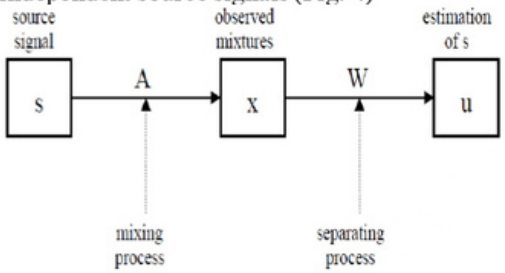


Fig. 4. Independent Source Signals

ICA goes one step further so that it transforms the whitened data into a set of statistically independent signals. While the basis images obtained are statistically independent, the coefficients that represent input images in the subspace defined by the basis images are not. The goal of ICA in is to find statistically independent coefficients for input data. In this architecture, the input is transposed, the pixels are variables and the images are observation. The source separation is performed on the pixels, and each row of the learned weight matrix $W$ is an image. A, the inverse matrix of $W$, contains the basis images in its columns. The statistically independent source coefficients in S that comprise the input images are recovered in the columns of $U$ (Fig. 4). This architecture was used to find image filters that produced statistically independent outputs from natural scenes. In this work, ICA is performed on the MRRILBP features rather than directly on the input images to reduce the dimensionality. The statistically independent coefficients are computed as $U = W * CT$ and the actual basis images shown in Fig. 5. Principal component analysis (PCA) is a popular example of such methods [16]. The basis images found by PCA depend only on pairwise relationships between pixels in the image database. In a task such as face

recognition, in which important information may be contained in the high-order relationships among pixels, it seems reasonable to expect that better basis images may be found by methods sensitive to these high-order statistics. Independent component analysis (ICA), a generalization of PCA, is one such method.

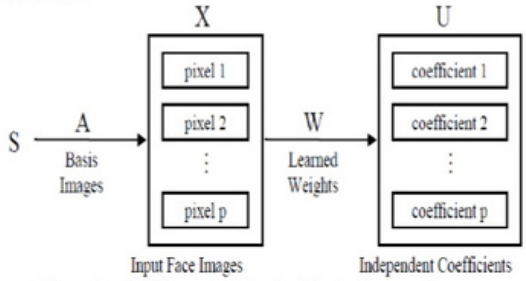


Fig. 5. Finding Statistically Independent Coefficients.

We used a version of ICA derived from the principle of optimal information transfer through sigmoidal neurons. ICA was performed on face images in the video database. ICA representations were superior to representations based on PCA for recognizing faces across high dimension and changes in pose. A classifier that combined the two ICA representations gave the best performance. To estimate Independent Components, $z$ should have nongaussian distribution, i.e. we should maximize nonguassianity. ICA is a proper to blind source separation or classification using ICs when class id of training data is not available. Regardless of which algorithm is used to compute ICA, there are two fundamentally different ways to apply ICA to VFR. The input face images in $X$ are considered to be a linear mixture of statistically independent basis images $S$ combined by an unknown mixing matrix $A$. The ICA algorithm learns the weight matrix $W$, which is used to recover a set of independent basis images in the rows of $U$. The face images are variables and the pixel values provide observations for the variables. The source separation, therefore, is performed in face space. Projecting the input images onto the learned weight vectors produces the independent basis images. The compressed representation of a face image is a vector of coefficients used for linearly combining the independent basis images to generate the image.

**Proposed Pose Invariant Video-Based Face Recognition System**

In this segment, we present the complete architecture of pose invariant face recognition system in Video. The proposed Pose Invariant Video-based Face Recognition System is as shown in Fig. 6. The proposed system consists of following modules; Video to frame conversion, face detection, face pose classification, feature extraction, feature reduction and feature matching. First module is video to frame conversion, for experiment purpose, five frames per video, second module is Face detection, it uses Viola Jones face detector, segmentation based technique for cropping the face from the background. Third module is face pose classification, in which it classify the poses in yaw, pitch and roll. In fourth module, we apply MRRILBP for feature extraction. In this approach the face image is divided into a small non-overlapping blocks or regions, where a histogram of the MRRILBP for each region (block) is constructed. The similarities of two images are then computed by summing the similarity of histograms from corresponding regions. For this reason, MRRILBP features are more suitable for face recognition across pose variations. In fifth module the features are reduced by ICA. In sixth module these reduced features are applied to the Euclidean distance classifier for matching. In order to evaluate the performance of our system, we use NRC-IIT [17], Honda-UCSD [18] and ORL [19] database. In order to evaluate the performance of our system, the details of each module are presented in the following subsections.

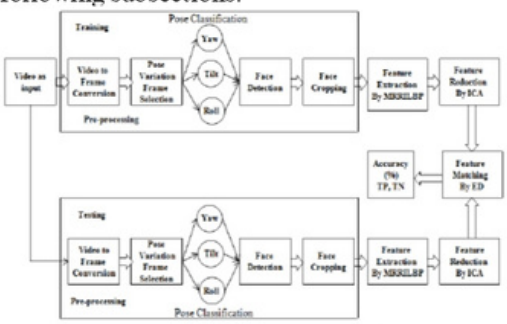


Fig. 6. Proposed Pose Invariant Video-based Face Recognition System

A. Face Detection

The process of locating the face in a given image and to separate it from the remaining background is called the face detection. Several approaches have been proposed to achieve this with different techniques [20]. Nevertheless, almost most approaches work effectively for frontal faces, where both the eyes are present in the face image. In contrast, if the performance of skin segmentation based face detection is investigated it proves to a larger degree of variation in poses. The main advantage of this method is that it can be applied to an image irrespective to the variation in poses of the image. After detecting the face next step is face cropping.

B. Pose Classification

Once the face is cropped from the input video frame/image, the pose classification of the face image is another most important module for our VFR system. It has been proved that each component contributes differently for the recognition when the pose combination of the matching pair is different. In this sense, a pose classification module could be used to decide the pose of test face images such that they are compared with the images with corresponding range of poses only, from one of the pose categories. This knowledge of pose of a test image aid in optimizing the search space and allows refining the search in particular pose category only. Thus, motivated with the face images, the poses of the input faces has been classified to one of the pose category (frontal profile, left profile and right profile). This assumption of three pose category could be used to map every input image with different poses that could alleviate the requirement of large number of samples per subject. The range of orientation angle we used to classify the pose is from $0^0$ by up to $90^0$.

C. Feature Extraction by MRRILBP

After the pose classification, to represent the face in terms of feature vector to make a machine learning model there is a need of feature extraction technique. In this fragment we discuss the feature extraction through MRRILBP (Fig. 7), this

approach is applied on cropped faces. Once the features have been extracted, we studied it for a large number of images with variation in poses. Similar effects are even observed on other angle metrics as the degree of orientation is moved from frontal to left or towards right. Our main objective is to present the fusion of MRRILBP in VFR, one to make the pose classification in the existence of vagueness/ambiguity in the data set and also independent of the presence of missing values. There in, the training observations from data set are assumed to belong to a finite set of pose category and we want to learn a classifier capable of assigning a test observation to one of the three pose categories (frontal profile, left profile, right profile).

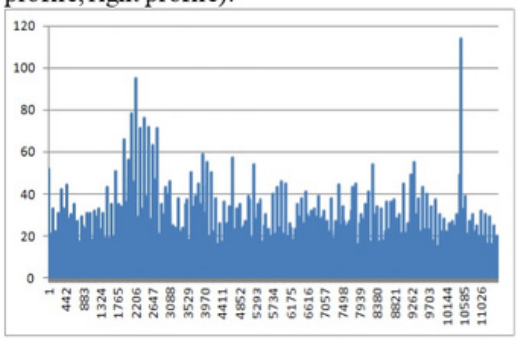


Fig. 7. MRRILBP Features of Honda-UCSD Video Database

D. Feature Reduction by Independent Component Analysis

Independent Component Analysis focuses on independent and non-Gaussian components, Higher-order statistics and Non-orthogonal transformation. A signal ( $X$ ) is generated by linear mixing ( $A$ ) of independent components ( $s$ ) ICA is a statistical analysis method to estimate those independent components ( $z$ ) and mixing rule ( $W$ ).

$$W * X = U = X = A * U \quad (9)$$

$$W^{-1} = A \quad (10)$$

In Independent Component Analysis a one variable cannot be estimated from other variables, it is independent. By Central Limit Theorem, a sum of two independent random variables is more Gaussian than original variables distribution of independent components are nongaussian. To estimate Independent Components, $z$ should have nongaussian distribution, i.e. we maximize non-guassianity.

E. Feature Matching by Euclidean Distance All the images are easily discussed in dimensional Euclidean space, called image space. It is natural to adopt the base to form a coordinate system of the image space, where it

corresponds to an ideal point source with unit intensity location. Thus an image is converted to the grey level at that pixel, is represented as a point in the image space, and is the coordinate with respect to that face image. The origin of the image space is an image whose grey levels are zero everywhere. Although the algebra of the image space can be easily formulated. The Euclidean distance of images (i.e. the distance between their corresponding points in the image space) could not be determined until the metric coefficients of the basis are given. The metric coefficients are defined as the scalar product and the angle. Note that, if all the base vectors have the same length, then it depends completely on the angle. Euclidean distance converts images into vectors according to grey levels of each pixel and then compares intensity differences pixel by pixel. Here we compare the MRRILBP features of test data with MRRILBP features of train data using Euclidean distance from which we recognize test video data with the help of video train data. The formula
to calculate Euclidean distance is given by,

$$d(x,y)=\sqrt{\sum_{i=1}^{k}(m_i-n_i)^2} \quad (11)$$

Where $m_i$ = train image pixel & $n_i$ = test image pixel

**Results and Discussion**

A. Algorithm

Input: Video clip $I(x,y)$ with a set of frame sequences.

Output: Recognized face $I'(x',y')$

Step 1. Pre-processing steps

_ Video clips to frame conversion.

_ Random selection of frames or images.

_ Conversion from RGB to grayscale.

_ Initialize median filter

Step 2: Face detection using vision.CascadeObjectDetector

Step 3: Face cropping from frame

Step 4: Apply MRRILBP texture classifier on cropped face $I(x,y)$

$$|H|+|L|=N$$

$$s(z)=\{1, z\geq 0$$

$$s(z)=\{1, z<0$$

where $s(z)$ is the thresholding (step) function

Step 5: Block per image are 20 X 26, sampling points 8 per
circle and radius of circle 2, 3, 4.

Step 6: Apply ICA for feature reduction.

$$W*X=UX+A*U$$

$$W^{-1}=A$$

Step 7: Apply Euclidean distance for matching the face frame

$I'(x',y')$ from the original input frame $I(x,y)$

$$d(x,y)=\sqrt{\sum_{i=1}^{k}(m_i-n_i)^2}$$

B. Experimental Data

In this section, we describe the data used in our experiments.

Typically, Video-based Face Recognition simultaneously involves three steps: segmentation, tracking and recognition of the faces. However, our goal in this approach is to analyse how to represent the faces for recognition and to develop a full video-based face recognition system. Therefore, we focus our experiments on the recognition phase, assuming that the faces are well segmented and tracked. Thus, we considered three different databases, ORL, Honda-UCSD and NRC-IIT database is the most commonly used database in video-based face recognition research [21], [22], [23]. The first database, Honda-UCSD, has been collected and used by K. C. Lee et al. in their work on video-based face recognition [24]. The database contains 40 video sequences of 20 different individuals (2 videos per person). During the data collection, the individuals were asked to move their face in different combinations (speed, rotation and expression). From the video face database, we have detected and cropped the face images. The size of the extracted face images is 20X26 pixels. NRC-IIT database consists of pairs of short video clips captured by an Intel web-cam mounted on the computer monitor. It shows a wide range of pose variations. ORL is a face image database; it includes the 40 folders containing 10 images in each. The database consists of total 400 images of male and female, with 10 poses within $\pm 20^0$ in yaw.

C. Face Learning from Videos

In face recognition schemes both training and test data (galleries and probes) are video

sequences. The recognition consists of matching the feature representation extracted from the probe videos to those extracted from the galleries. In order to check whether a feature representation enhances face recognition performance, one should compare the results to those obtained using still-image-based techniques under the same conditions. In this approach, we have done the experiment on video databases. In this experiment, we have taken selected frames of pose variation of major angle from all videos of databases, advantage is recognition time and memory space required is less, accuracy is (ORL $\pm 20^0$, NRCIIT $\pm 90^0$, Honda-UCSD $\pm 90^0$) 96.9%. As shown in the TABLE I and Fig. 9, the approach of PCA [25] (89.5%), LBP [26] (69.02%), modified Log gabor + rmf [14] (76%) methods on different databases. This confirms that the dynamic information supports the face recognition process. In the some previous methods, the pose variation angle is $\pm 20^0$ for image face database. Xiaoying Wang et. al proposed a novel approach called coupled kernel-based enhanced discriminant analysis (CKEDA), pose variation angle is $\pm 30^0$. CKEDA aims to simultaneously project the features from LR non-frontal probe images and HR frontal gallery ones into a common space where discrimination property is maximized [27] and it's recognition rate is 89%. Annan Li et. al proposed a new approach for cross-pose face recognition using a regressor with a coupled bias-variance tradeoff, pose variation angle is $\pm 90^0$. They found that striking a coupled balance between bias and variance in regression for different poses could improve the regressor- based cross-pose face representation, i.e., the regressor can be more stable against a pose difference. With the basic idea, ridge regression and lasso regression are explored [28], its recognition rate is 73.52%. Huy Tho Ho et.al present a method for reconstructing the virtual frontal view from a given nonfrontal face image using Markov Random Fields (MRFs) and an efficient variant of the Belief Propagation (BP) algorithm [3], pose variation angle is $\pm 40^0$ and it's recognition rate is 91.5%. Haoxiang Li and Gang Hua approach this problem through a probabilistic elastic part model. They extract local descriptors (e.g., LBP or SIFT) from densely sampled multi-scale image patches, pose variation angle is $\pm 90^0$. By augmenting each descriptor with its location, a Gaussian mixture model (GMM) is trained to capture the spatial-appearance distribution of the face parts of all face images in the training corpus, namely the probabilistic elastic part (PEP) model. Each mixture component of the GMM is confined to be a spherical Gaussian to balance the influence of the appearance and the location terms, which naturally defines a part [29], it's recognition rate is 88.04%. Zahid Mahmood, Tauseef Ali and Samee U. Khan present a comparative study of three baseline face recognition algorithms to analyse the effects of two aforementioned factors, pose variation angle is $\pm 30^0$. The algorithms studied include (a) the adaptive boosting (AdaBoost) with linear discriminant analysis as weak learner,

(b) the principal component analysis (PCA)-based approach,

and (c) the local binary pattern (LBP)-based approach. They perform an empirical study using the images with systematic pose variation and resolution from multi-pose, illumination, and expression database to explore the recognition accuracy [30], it's recognition rate is 60%. A novel method for face recognition under pose and expression variations is proposed by Ali Moeini and Hossein Moeini [31] from only a single image in the gallery, pose variation angle is $\pm 90^0$. A 3D Probabilistic Facial Expression Recognition Generic Elastic Model (3D PFER-GEM) is proposed to reconstruct a 3D model from real-world human face using only a single 2D frontal image with/without facial expressions. Then, a Feature Library Matrix (FLM) is generated for each subject in the gallery from all face poses by rotating the 3D reconstructed models and extracting features in the rotated face pose, it's recognition rate is 91.90%. A novel pose-invariant face recognition method is proposed by Poonam Sharma et. al by combining curvelet invariant moments with curvelet neural network, pose variation angle is $\pm 40^0$. First a special set of statistical coefficients using higher-order moments of curvelet are extracted as the feature vector and then the invariant features are fed into curvelet

neural networks [12], it's recognition rate is 86.6%. Ying Tai et. al introduce the orthogonal Procrustes problem (OPP) as a model to handle pose variations existed in 2D face images. OPP seeks an optimal linear transformation between two images with different poses so as to make the transformed image best fits the other one [32], pose variation angle is $\pm 45^0$ and its recognition rate is 96.8%. Xi Yin and Xiaoming Liu explores Multi-Task Learning (MTL) for face recognition. First, they propose a multi-task Convolutional Neural Network (CNN) for face recognition where identity classification is the main task and Pose, Illumination and Expression (PIE) estimations are the side tasks [33], pose variation angle is $\pm 90^0$ and its recognition rate is 91.1%. In our system, we have trained the frontal profile frames and test the frames of $\pm 90^0$ pose variations (Fig. 8). As compared to other systems, we have got the best accuracy (95% to 96.9%) for $\pm 90^0$

Table I - Comparison Of Recognition Rates Of Different Methods

| Algorithm | Pose variation angle | Recognition rate |
|---|---|---|
| Modified log Gabor + rmf [14] | $\pm 20^0$ | 76% |
| PCA [25] | $\pm 20^0$ | 89.5% |
| LBP [26] | $\pm 20^0$ | 69.02% |
| CKEDA [27] | $\pm 30^0$ | 89.0% |
| Adaboost+LDA [30] | $\pm 30^0$ | 60% |
| MRF+BP [3] | $\pm 40^0$ | 91.5% |
| CNN [12] | $\pm 40^0$ | 86.6% |
| OPP [32] | $\pm 45^0$ | 91.7% |
| Stacked OPP [32] | $\pm 45^0$ | 96.8% |
| CBVT [28] | $\pm 90^0$ | 73.52% |
| LBP+GMM+PEP [29] | $\pm 90^0$ | 88.04% |
| FLM+PFER-GEM [31] | $\pm 90^0$ | 91.90% |
| P-CNN [33] | $\pm 90^0$ | 91.1% |
| MRRILBP (Proposed approach) | $\pm 90^0$ | 96.9% |


Fig. 8. A: Frontal Frames for Training Purpose. B: Non-Frontal Frames forTesting Purpose ( $\pm 90^0$ ).

video face database. In video database the adjacent frames have no major change in pose, so for testing purpose we have consider the selected frames with major change in pose variation. One more novelty of this system is that, we can recognise the face in minor to major pose variation angle. We propose a pose invariant VFR system based on MRRILBP for Video face databases. We apply MRRILBP for feature extraction; the motivation behind using MRRILBP is that, it is one of the good algorithms that deal with Video-based face recognition. The face image or frame is divided into a small non-overlapping blocks or regions, where a histogram of the MRRILBP for each region (block) is constructed. The similarity of two images are then computed by summing the similarity of histograms from corresponding regions. For this reason, MRRILBP features are more suitable for face recognition across pose variations. Feature reduction by ICA. These features are applied to the euclidean distance classifier for recognition.

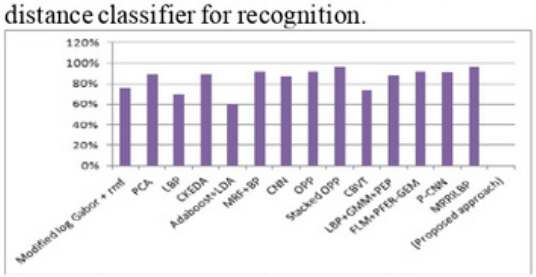


Fig. 9. % Accuracy Comparison Graph for Different Methods

**Conclusion**

In this paper, we have proposed a new algorithm of Multi-Radius Rotation Invariant Local Binary Pattern (MRRILBP). To train the models, we have taken frontal faces for training purpose and for testing $90^0$ pose variation faces; still our system gives better results. For experiment purpose we have taken the selected frames for testing (Major pose variation angle) of video database which uses both spatial and dynamic information and then apply the MRRILBP algorithm. We have performed extensive experiment on three different databases. The MRRILBP outperformed than other previous methods.

**References**


1. Simone K. Favelle and Stephan Palmisano,"The Face Inversion Effect Following Pitch and Yaw Rotations: Investigating the Boundaries of Holistic Processing", Published online 2012 Dec 18. doi: 10.3389/fpsyg.2012.00563, Vol.3, article no. 563, 2012.
2. Himanshu S. Bhatt, Richa Singh and Mayank Vatsa, "On Recognizing Faces in Videos Using Clustering-Based Re-Ranking and Fusion", IEEE Transactions on Information Forensics and Security, vol. 9, Issue: 7, pp. 1056-1068, 2014.
3. Huy Tho Ho and Rama Chellappa,"Pose-Invariant Face Recognition Using Markov Random Fields",IEEE Transactions on Image Processing, Vol. 22, Issue 4, pp. 1573- 1584, 2013.
4. Utsav Prabhu, Jingu Heo and Marios Savvides,"Unconstrained Pose-Invariant Face Recognition Using 3D Generic Elastic Models", IEEE Transactions on Pattern Analysis and Machine Intelligence, Vol. 33, Issue 10, pp. 1952 - 1961, 2011.
5. Richa Singh, Mayank Vatsa, Arun Ross and Afzel Noore,"A Mosaicing Scheme for Pose-Invariant Face Recognition", IEEE Transactions on Systems, Man, and Cybernetics, Part B (Cybernetics), Vol. 37, Issue 5, pp. 1212 - 1225, 2007.
6. David J. Beymer,"Face recognition under varying pose", Technical Report 1461, MIT AI Laboratory, Cambridge, MA, 1993.
7. A. Pentland, B. Moghaddam and T. Starner,"View-based and modular eigenspaces for face recognition", In Proceedings of the IEEE Conference on Computer Vision and Pattern Recognition, pp. 8491, 1994.
8. M. Turk and A. Pentland,"Face recognition using eigenfaces", In Proceedings of the IEEE Conference on Computer Vision and Pattern Recognition, 1991.
9. Xi Yin and Xiaoming Liu, "Multi-Task Convolutional Neural Network for Pose-Invariant Face Recognition", IEEE Transactions on Image Processing, DOI: 10.1109/TIP.2017.2765830, Vol. 27, Issue: 2, pp. 964-975, 2017.
10. Manar D. Samad and Khan M. Iftekharuddin, "Frenet Frame-Based Generalized Space Curve Representation for Pose-Invariant Classification and Recognition of 3-D Face", IEEE Transactions on Human-Machine Systems, Vol. 46, Issue: 4, pp. 522-533, 2016.
11. Changxing Ding, Chang Xu and Dacheng Tao, "Multi-Task Pose-Invariant Face Recognition", IEEE Transactions on Image Processing, DOI: 10.1109/TIP.2015.2390959, Vol. 24, Issue: 3, pp. 980-993, 2015.
12. Poonam Sharma, Ram N. Yadav and Karmveer V. Arya, "Pose-invariant face recognition using curvelet neural network", IET Biometrics, DOI: 10.1049/iet-bmt.2013.0019, Vol. 3, Issue 3, pp. 128-138, 2014.
13. Sihao Ding, Ying Li, Junda Zhu, Yuan F. Zheng and Dong Xuan, "Sequential Sample Consensus: A Robust Algorithm for Video-based Face Recognition", IEEE Transactions on Circuits and Systems for Video Technology, vol. 25, issue 10, pp. 1586-1598, Oct. 2015.
14. Singh Kavita, Zaveri Mukesh and Raghuwanshi Mukesh,"Rough set based pose invariant face recognition with mug shot images", Journal of Intelligent and Fuzzy Systems: Applications in Engineering and Technology archive, vol. 26, Issue 2, pp. 523-539, March 2014.
15. Ahonen T., Matas J., He C. and Pietikinen M., "Rotation invariant image description with local binary pattern histogram Fourier features", Scandinavian Conference on Image Analysis, Lecture Notes in

Computer Science, vol. 5575, pp. 61-70, Springer, Berlin, 2009.
16. A. Hadid and M. Pietikainen. "From Still Image to Video-Based Face Recognition: An Experimental Analysis", Automatic Face and Gesture Recognition, 2004. Proceedings. Sixth IEEE International Conference, 2004.
17. http://www.videorecognition.com/db/video/faces/cvglab/avi/
18. vision.ucsd.edu/leekc/HondaUCSDVideoDatabase/HondaUCSD
19. http://www.cl.cam.ac.uk/research/dtg/attarchive/facedatabase
20. Paul Viola and Michael Jones, "Robust Real-Time Face Detection", International Journal of Computer Vision, Kluwer Academic Publishers. Manufactured in The Netherlands, vol. 57, no. 2, pp. 137-154, 2004.
21. S. Zhou and R. Chellappa, "Probabilistic human recognition from video", in Proceedings of the European Conference on Computer Vision, Copenhagen, Denmark, pp. 681-697, 2002.
22. X. Liu and T. Chen, "Video-based face recognition using adaptive hidden markov models", In Proc. of IEEE Int. Conf. on Computer Vision and Pattern Recognition, pp. 340-345, 2003.
23. V. Kruger and S. Zhou, "Exemplar-based face recognition from video", in Proceedings of the European Conference on Computer Vision, Copenhagen, Denmark, pp. 361-365, 2002.
24. K. C. Lee, J. Ho, M. H. Yang and D. Kriegman, "Videobased face recognition using probabilistic appearance manifolds", in Proceedings of IEEE Computer Society Conference on Computer Vision and Pattern Recognition, pp. 313-320, June 2003.
25. D. Demers and G. W. Cottrell, "Non-linear Dimensionality Reduction", In Advances in Neural Information Processing Systems, pp. 580-587, 1993.
26. K. Jaya Priya and R.S. Rajesh, "A local min-max binary pattern based face recognition using single sample per class", International Journal of Advanced Science and Technology, vol.36, pp. 41-50, 2011.
27. Xiaoying Wang, Haifeng Hu and Jianquan Gu, "Pose robust low-resolution face recognition via coupled kernel based enhanced discriminant analysis", IEEE/CAA Journal of Automatica Sinica, vol. 3, Issue. 2, April 2016.
28. Annan Li, Shiguang Shan and Wen Gao, "Coupled BiasVariance Tradeoff for Cross-Pose Face Recognition", IEEE Transactions on Image Processing, vol. 21, Issue. 1, Jan. 2012.
29. Haoxiang Li and Gang Hua, "Probabilistic Elastic Part Model: A Pose-Invariant Representation for Real-World Face Verification", IEEE Transactions on Pattern Analysis and Machine Intelligence, vol. 40, Issue. 4, pp. 918-930, April 2018.
30. Zahid Mahmood, Tauseef Ali and Samee U. Khan, "Effects of pose and image resolution on automatic face recognition", IET Biometrics, vol. 5, Issue: 2, pp. 111-119, 2016.
31. Ali Moeini and Hossein Moeini, "Real-World and Rapid Face Recognition Toward Pose and Expression Variations via Feature Library Matrix", IEEE Transactions on Information Forensics and Security, vol. 10, Issue. 5, pp. 969-984, 2015.
32. S. T. Jagtap, C. M. Thakar, O. El imrani, K. Phasinam, S. Garg and R. J. M. Ventayen, "A Framework for Secure Healthcare System Using Blockchain and Smart Contracts," 2021 Second International Conference on Electronics and Sustainable Communication Systems (ICESC), 2021, pp. 922-926, doi: 10.1109/ICESC51422.2021.9532644.
33. Ying Tai, Jian Yang, Yigong Zhang, Lei Luo, Jianjun Qian and Yu Chen, "Face Recognition With Pose Variations and Misalignment via Orthogonal Procrustes Regression", IEEE Transactions on Image Processing, vol. 25, Issue. 6, pp. 2673-2683, 2016.
34. Xi Yin and Xiaoming Liu, "Multi-Task Convolutional Neural Network for Pose-Invariant Face Recognition", IEEE Transactions on Image Processing, vol. 27, Issue. 2, pp. 964-975, 2018.
35. Ruxandra Tapu, Bogdan Mocanu and Titus Zaharia, "DEEP-HEAR: A Multimodal Subtitle Positioning System Dedicated to Deaf and Hearing-Impaired People", May 2019.
36. Weiwei Wang, Xiaoyan Chen, Shuangwu Zheng and Haiqing Li, "Fast Head Pose Estimation via Rotation- Adaptive Facial Landmark Detection for Video Edge Computation", IEEE journal on Special Section on Innovation and Application of Intelligent Processing of Data, Information And Knowledge as Resources in Edge Computing, March 2020.

Science and Technology Journal Vol. 10 Issue: 1 January 2022 ISSN: 2321-3388

# UWB BPF Using Hybrid Microstrip CPW with DGS Structure for Future Wireless Communication

**Jagadish Baburao Jadhav[1*], Sagar Arun More[2], Vijay Shrinath Patil[3], Kiran Hilal Sonawane[4], Vaishali B Patil[5], Pravin Sahebrao Patil[6]**

[1, 2, 3, 4] Department of Electronics and Telecommunication Engineering. R. C. Patel Institute of Technology, Shirpur-425405, India.

[5]Department: Master of Computer Applications. R. C. Patel Educational Trust's, Institute of Management Research and Development, Shirpur-425405, India.

[6]Department of Electronics and Telecommunication Engineering. S. S. V. P. S. B. S. Deore COEngineering, Dhule-424005, India.

[*]Email: jagadish.jadhav@rcpit.ac.in, jagadish.rcpit@gmail.com

**Abstract—**The aim of this paper is to design Ultra-Wide Band (UWB) Band Pass Filter (BPF) based on the microstrip-to-Coplanar Waveguide (CPW) transitions. UWB BPF using hybrid microstrip CPW and Defected Ground Structure (DGS) have been proposed and developed. Till now, few techniques are invented for designing UWB bandpass filter. One amongst these techniques is Hybrid Structure of two different planar transmission lines i.e. microstrip and coplanar waveguide are used. Compactness can be achieved by using this technique. A more flexible structure in terms of geometrical dimensions for getting optimum performance are obtained for planar circuit implementation. This is feasible thanks to the simultaneous use of microstrip and coplanar waveguide technologies. These qualities makes this technique superior over the other techniques. A detail experimental work of UWB B is presented in this paper. Alongside, the design and analysis of three (design 1, design 2 and design 3) UWB BPF structures is carried out. The UWB bandpass filter design gives a return loss less than -20 dB, flat group delay, very less insertion loss at every frequency point within whole UWB. These filter are useful alternative to other recently proposed structures in the literature.

**Keywords:** Coplanar Waveguide (CPW), Bandpass Filter (BPF), Coplanar Waveguide (CPW), Insertion Loss, Return Loss, Electromagnetic coupling, Defected Ground Structure (DGS), Transmission Zeros (TZs).

## INTRODUCTION

Federal Communication Commission (FCC) sanctioned the unlicensed use of frequency band starting from 3.1 GHz to 10.6 GHz as Ultra-Wideband (UWB). For commercial communication applications in February 2002, the UWB radio system has been receiving great attention and gaining momentum from both academy as well as industry. A major device among many passive components is a bandpass filter design. In (Zhang et al. 2019) Five BPF is used to obtain UWB design by increasing or decreasing BPF in parallel according to requirement for electromagnetic acoustic signal detection. In (Bohra et al. 2020) a single notch band BPF with & without DGS technology is used which includes a pair of spiral shaped & H- slot resonators which gives good results. In (Raghava et al. 2021) proposed planer UWB BPF with two transmission zeros & DGS with complimentary split ring resonator & complementary folded split ring resonator. In (Karimi et al. 2019) designed compact narrow BPF in which two independently fully controllable passbands are used using two different coupling paths, got good simulation & measured results at 3.5 & 5.8 GHz with FBW 0.8% & 1%. In (Ghazali et al. 2018) a compact dual notch band UWB BPF is discussed. BPF is designed using microstrip to CPW


https://doi.org/10.22232/stj.2021.09.02.01

technology. CPW is short circuited at ground & vertically connected to microstrip lines through dielectric. In (Wu et al. 2021) Nine high performance resonant modes are generated using direct connected T- shaped stub loaded resonator with three bands having FBW 65%, 42% and 31% and return loss of 42.9, 44.5 and 42.9 decibal. In (Sakotic et al. 2017) UWB BPF designed using circular patch resonator grounded via and unsettled by slits and DGS. This design is simulated, fabricated and measured, got outperforms compared with other UWB filters. In (Ghazali et al. 2017) broadside coupling of microstrip and coplanar waveguide is used. CPW is embedded in ground plane so that gives equispace resonant modes in UWB range. Four open ended stubs are appended on top to improve the performance. In (Bakali et al. 2020) microstrip coplanar waveguide microstrip transition is used, which gives good agreement between measurement and simulation results. In (Bakali et al. 2019) low budget FRP-4 is used, a flat group delay performance was obtained with variation of 0.15nS over the bandwidth suitable for wireless UWB devices as in (Bakalia et al. 2020) group delay about 0.22nS. In (Luo et al. 2010) a quasi-elliptic response and multi-mode UWB performance are obtained through DMR and transition from microstrip to CPW, mode stepped impedance resonator is used in (Wu et al. 2019). To obtain novel results a contiguous and concentric split ring resonators and ring resonators are used in (Mukherjee et al. 2017). A sharp out of band rejection performance is achieved in (Guo et al. 2015), triple mode stepped impedance resonator (Liu et al.2018) gives advantage to higher degree of freedom to adjust resonant frequencies. In (Gupta et al. 2017) triple notch UWB filter is designed using short circuit stubs and defected microstrip line structure. In (Hao et al. 2010), a wide array of novel and creative techniques to design an UWB bandpass filter is being reported. Fractional bandwidth is defined as absolute bandwidth divided by the center frequency. The fractional bandwidth is a better measure for bandwidth when comparing different antennas and filters because it is independent of scale:

$$Bf = 2\left(\frac{fh - fl}{fh + fl}\right) \quad (1)$$

Where fh is higher cutoff frequency and fl is lower cutoff frequency of passband. Normally this is defined as the range of the frequencies over which the return loss is acceptable. The detail literature can be seen from (Jadhav et al.2017).

Major contributions of this paper are:

1) Authors improved the Return loss ($S_{11}$).
2) Insertion loss ($S_{21}$) parameters of the filter, with DGS.
3) The parameters extraction using mathematical modelling of symmetrical networks for even mode and odd mode.
4) The design 1, design 2 and design 3 of UWB BPF structures with DGS exhibit a simple planar structure, compact size, resonance modes within the passband as well as independent of ground plane size and radiation pattern without supplementary circuit space.

The simulation results coming very good as Return loss $S_{11}$ is flat to 20 dB, previously compaired to without DGS. The simulation results of (design 1, design 2 and design 3) UWB BPF structures with DGS are coming very good as Return loss $S_{11}$ is steady and consistent to 20 dB. Such filters are suitable for use in (Jadhav et al.2017).

## DESIGN 1: UWB BPF BASED ON HIGH PASS FILTER PROTOTYPE

The microstrip-to CPW transition arrangement in Figure 2 is adjusted to build a changeover stub of dimension w4, as shown in Figure 2. The dimensions for Figure 2 can be seen from the calculations: d1 = 0.038 cm, d2 = 0.05 cm, d3 = 0.0635 cm, and d4 = 0.028 cm. w1 = 8.9 cm, w2 = 0.381 cm, w3 = 0.559 cm, w4 = 0.0635 cm, w5 = 0.038 cm, w6 = 0.152 cm, and w7 = 0.521 cm.

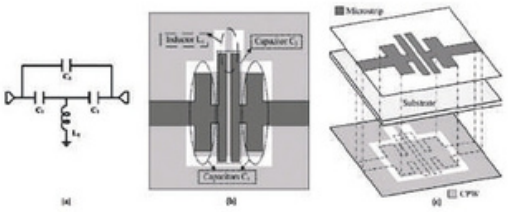

**Fig. 1: (a) HPF Prototype with Capacitor $C_2$ (b) HPF Realized with Microstrip and CPW (c) 3-D View.**

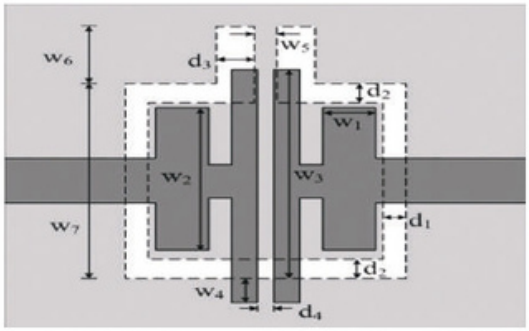


**Fig. 2: Circuit Arrangements of Three-Pole UWB Bandpass Filter with Dimensions.**

## Design 1: Analysis of Symmetrical Network

As the circuit is symmetrical, even-odd mode investigation technique can be used to analyze the circuit. So, bisecting the circuit into two identical halves acting as a single port network individually. The bisected circuit diagram is shown in Figure 3.

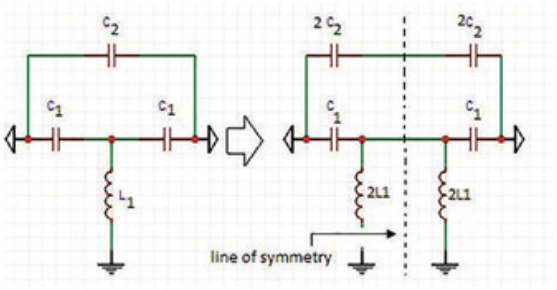


**Fig. 3: Symmetrical Network.**

Under even mode, line of balance acts as an open circuit as shown in Figure 4(a). Hence, capacitor $C_2$ will be disconnected from circuit.

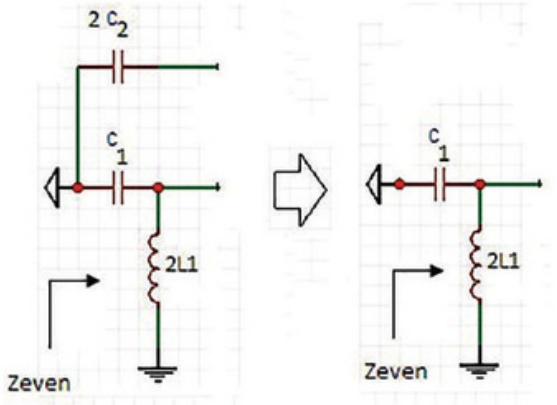


**Fig. 4: (a) Even Mode Impedance (b) Odd Mode Impedance of Symmetrical Network.**

This Even & Odd symmetric circuit decomposition technique removes the basic need for the RF designer to perform further simulations to obtain the even-mode and odd-mode circuits once the complete circuit S-parameters are known (Roberg et al. 2013). Conventionally $Z_{even}$ and $Z_{odd}$ are computed using equation given below.

$$Z_{even} = R + jX \quad (2)$$

$$Z_{even} = 0 + j\,(X_L - X_C) \quad (3)$$

$$Z_{even} = j\,(2wL_1 - 1/wC_1) \quad (4)$$

Underneath odd mode, line of symmetry acts as a short circuit as shown in 4.4(b). Hence, capacitor $L_1$ will be shorted.

$$Z_{odd} = R + jX \quad (5)$$

$$Z_{odd} = 0 + j(X_L - X_C) \quad (6)$$

$$Z_{odd} = (1/jw\,(C_1 + 2C_2)) \quad (7)$$

A transmission zero is produced when the transfer function $S_{21}$ is identical to zero, i.e.

$$Z_{even} = Z_{odd} \quad (8)$$

The width of input and output microstrips are calculated in a way so that the microstrips can have a characteristics impedance of 50 ohm in order to have a proper impedance matching when used in application circuit. Substrate height is taken equal to 0.508 mm and dielectric constant of 3.38. Thus using this data and equation, effective dielectric constant and characteristics impedance are calculated. The thickness of input as well as output microstrips is designed for the characteristics impedance to be 50Ω. The calculated width is 1 mm.

## Design 1: Simulation Result

Mentor graphics HyperLynx IE3D electromagnetic simulator is used for design, edit and simulation purpose. IE3D software uses method of moments for analysis of structure (Mentor Graphics Manual 2020). The scattering parameters i.e. S-parameters are used to analyze the filter performance. Transmission coefficient is characterized by insertion loss ($S_{21}$) and reflection coefficient is characterized by return loss i.e. ($S_{11}$). The S-parameter graph is shown in Figure 5. The 10 dB bandwidth is from 3.29 GHz to 8.00 GHz. Thus the passband width is 4.71 GHz. The fractional bandwidth is 78.5%. Figure 6 shows current distribution of design 1. Current is flowing through the filter structure with 18 dB loss. The in-band return and insertion losses are good (i.e.$|S_{11}| \geq$ -20 dB, and $|S_{21}| \leq -1$ dB) with frequency selectivity at both edges is high. The green line indicates the $S_{21}$ and other colour line indicates the $S_{11}$ as shown in Figure 5. The practical $S_{11}$ and $S_{21}$ response shows even better agreement with the calculation.

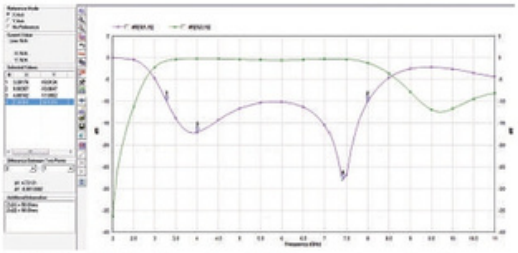

**Fig. 5: Simulation Results of S-Parameters $S_{11}$ Vs. Operating Frequency of Design 1.**

Figure 7 shows group delay of design 1. Group delay is constant in the UWB. The filter reported in design 1 has very good selectivity. Poles has been seen at the start of UWB and at the end of UWB to improve the selectivity of the filter.

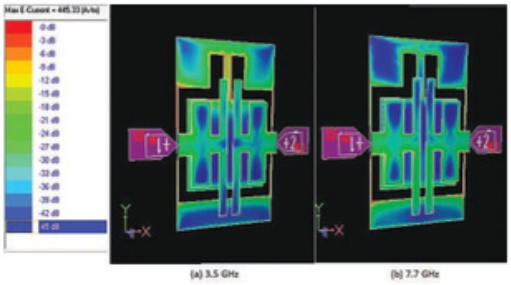


**Fig. 6: Simulation Results of Current Distribution Vs. Operating Frequency of Design 1.**

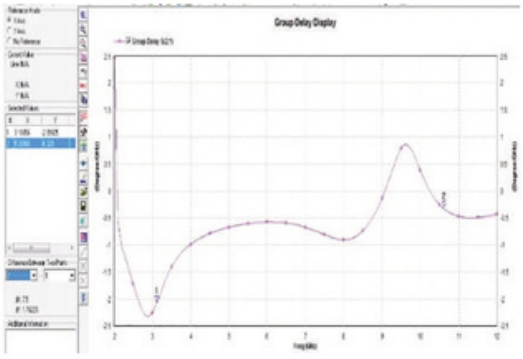

**Fig. 7: Simulation Results of Group Delay Vs. Operating Frequency of Design 1.**

## DESIGN 2: UWB BPF WITH MULTIPLE RESONATING STRUCTURE

A CPW non uniform resonator or multiple-mode resonator (MMR) is created. In this design, the UWB filter is designed by taking substrate of relative dielectric constant of 10.8 and thickness of 0.635 mm.

**Table 1: Frequencies of Resonance are Determined (f1, f2, f3) with (S1) for the Multi-Mode Resonator in Figure 9.**

| S1 | 0.18 | 0.58 | 0.98 | 1.10 | 1.38 | 1.78 |
|---|---|---|---|---|---|---|
| *f1(GHz)* | 3.67 | 4.01 | 4.12 | 4.13 | 4.15 | 4.16 |
| *f2(GHz)* | 7.29 | 7.10 | 6.84 | 6.76 | 6.60 | 6.34 |
| *f3(GHz)* | 10.91 | 10.12 | 9.55 | 9.40 | 9.13 | 8.74 |

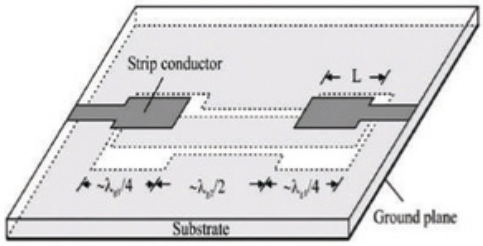


**Fig. 8: Schematic of UWB BPF (Design 2).**

Figure 9(a) shows, the open-ended multi-mode resonator. Figure 9(b) shows its equivalent circuit. Here, Yi = 0 for calculations of resonant modes frequencies. Figure 10(a) shows a hybrid microstrip/CPW surface-to-surface connection. Its coupling may emphasized in terms of a parallel J-inverter series as illustrated in Figure 10(b). The three stubs in CPW are grounded to the common ground of CPW. There are two microstrip open-circuited stubs on top side of common substrate. These microstrip open-circuited stubs are separated by a gap g1. A vertical coupling between top microstrip stub and bottom CPW side stubs is achieved. The dimensions for the structure are shown in figure 10.

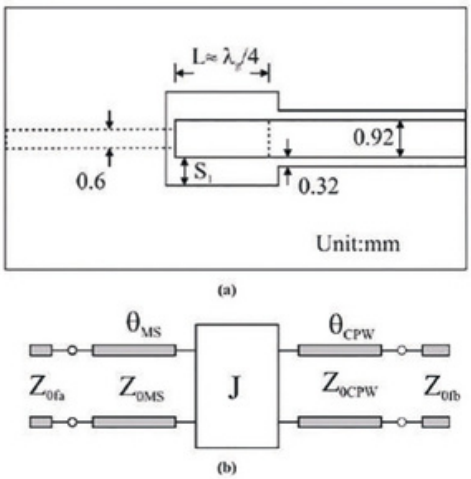


**Fig. 9: MMR on Coplanar Waveguide Transition (a) Design. (b) Corresponding Network.**

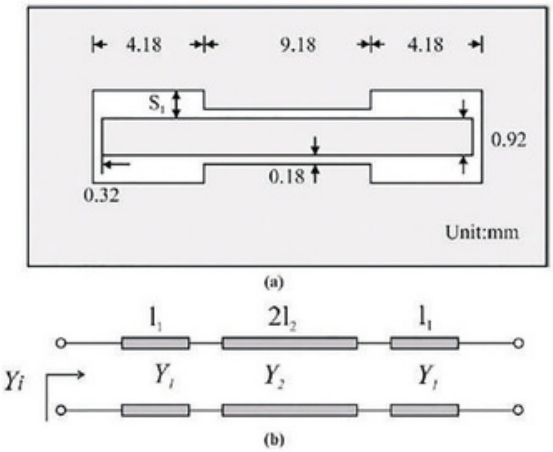


**Fig. 10: Layout of Microstrip/CPW Connection (a) Design with Dimensions. (b) Corresponding J-Inverter Setup.**

## Design 2: Simulation Result

The insertion loss is flat and closer to 0-dB line and return loss is below -10 dB line as shown in Figure 11. The 10 dB bandwidth starts from 2.99 GHz to 10.55 GHz. The width of passband is (10.55-2.99) = 7.56 GHz. The FBW is 111.69%. The filter structure in design 2 gives five transmission poles. The electromagnetic simulation software used for designing and simulating the filter structure is Mentor Graphics Hyperlynx IE3D (Mentor Graphics Manual 2020). It uses the method of moment to analyse the structure. Figure 3 shows how a filter structure looks in IE3D Mgrid editor. The yellow part shows open-circuited microstrip stubs and green part shows CPW. The finite ground plane provided by IE3D is used for designing and simulating the filter. So, differential ports are deployed for input output. The simulation results are shown in Figure 4. The transmission response i.e. insertion loss is predicted from $S_{21}$ and return loss is predicted from $S_{11}$. As can be seen from results, five transmission poles are obtained within UWB. The $S_{21}$ is very close to the 0 dB line within desired band that means insertion loss arised due to filter is very minimum. The $S_{11}$ is staying below -15 dB line this means a negligible amount of power is reflecting back to the port. The in-band return and insertion losses are good (i.e. $|S_{11}| \geq -10$ dB, and $|S_{21}| \leq -1$ dB) with frequency selectivity at both edges is high. The green line indicates the $S_{21}$ and other colour line indicates the $S_{11}$ as shown in Figure 11.

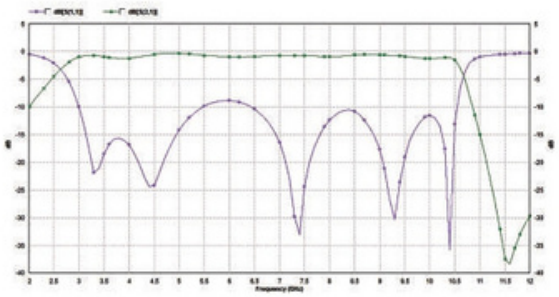

**Fig. 11: Simulation Results of S-Parameters $S_{11}$ Vs. Operating Frequency of Design 2.**

The current distribution of design 2 is shown in Figure 12. The surface current spreading at 3.3, 4.4, 7.3, 9.2 and 10.3 GHz the surface current density is largely concentrated in the ground plane around the hybrid microstrip coplanar waveguide. The current is flowing through the filter at resonant frequencies with 12 dB loss which is negotiable. Group delay is shown in Figure 13 it ranges between 0.46 to 0.74 ns, with the peak deviation of 0.30 ns over the entire UWB passband.

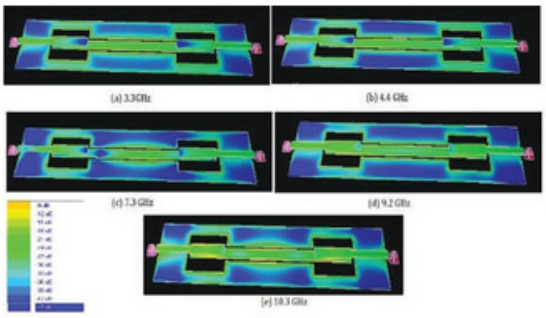

**Fig. 12: Simulation Results of Current Distribution Vs. Operating Frequency of Design 2.**

## DESIGN 3: UWB BPF WITH CPW QUARTER WAVELENGTH RESONATOR

The top microstrip structure and bottom CPW structure are electromagnetically coupled for signal energy transfer from input port to output port. The central conducting strip of conventional coplanar waveguide is customized to get three stubs. In this way, three stubs are designed within coplanar waveguide. These stubs are having their length quarter of the guided wavelength at the center frequency. Among these three stubs, two side stubs are of equal length while the central stub has length shorter than the two side stubs as shown in Figure 13. The filter is designed with a substrate having relative dielectric constant of 3.05 and a depth of

0.0508 cm. Proper results can be obtained for the dimensions, W2 = 0.14 cmm, d1 = 0.02 cm, d2 = 0.06 cm, g1 = 0.24 cm. W0 = 0.12 cm, L1 = 0.62 cm, L2 = 0.88 cm, W1 = 0.08 cm, the substrate parameters for designing filter are dielectric constant ε = 3.38, thickness (h) = 0.508 mm, tan δ = 0.002. The width W0 is taken as 0.12 cm for getting 50 Ω impedance. It can be calculated using formula in (Jadhav et al.2017). It solely depends upon effective dielectric constant, thickness h of substrate. Using CPW multiple resonating structure, three transmission poles can be obtained and to make band as flat as possible, top open circuited microstrips are designed which in turn to lead a five pole structure as a whole.

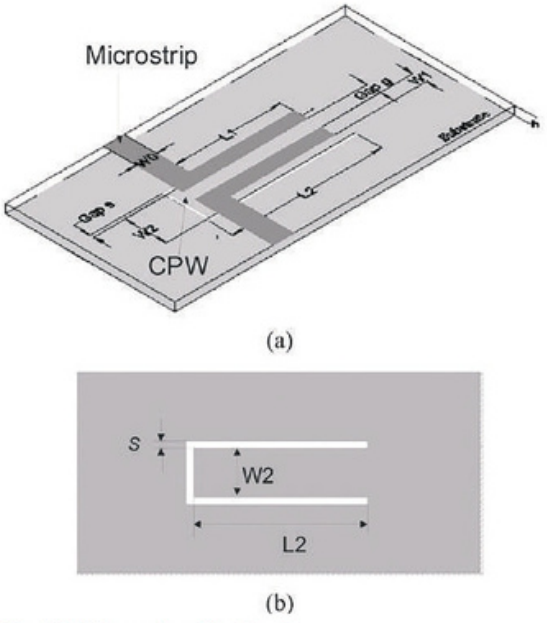


**Fig. 13: Schematic of Design 3.**

## Design 3: Simulation Result

Figure 15 shows the simulation result of design 3. The BPF gives a FB of 90 percent at a center frequency of 5.4, as well as poles at 1.95 and 10.36. The proposed filter can find the application in 5G and 6G tranreceiver front end design technology to achieve ubiquitous communications. Figure 16 shows current distribution at resonant frequencies. Figure 14 shows how a filter structure looks in IE3D Mgrid editor. The yellow part shows open-circuited microstrip stubs and green part shows CPW. The finite ground plane provided by IE3D (Mentor Graphics Manual 2020) is used for designing and simulating the filter. So, differential ports are deployed for input output. The simulation results are shown in Figure 15. The transmission response i.e. insertion loss is predicted from $S_{21}$ and return loss is predicted from $S_{11}$. As can be seen from results, five transmission poles are obtained within UWB. The $S_{21}$ is very close to the 0 dB line within desired band that means insertion loss arised due to filter is very minimum. The $S_{11}$ is staying below -15 dB line this means a negligible amount of power is reflecting back to the port. Further changes in design can be made with the help of optimization. By deciding optimization parameters, optimum performance can be obtained using optimization process. Taking into account the constant technological advances in the field of wireless communication devices and services, we can further modify the proposed design by making changes in CPW structure. To achieve this, slots, DGS, quasilumped elements can be utilized.

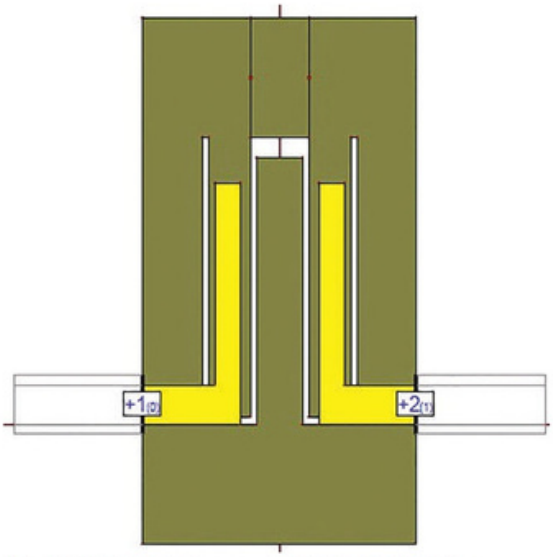

**Fig. 14: UWB BPF Structure in IE3D MGRID Editor.**

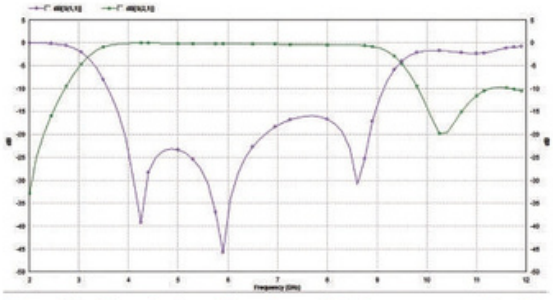

**Fig. 15: Simulation Results of S-Parameters $S_{11}$ Vs. Operating frequency of Design 3.**

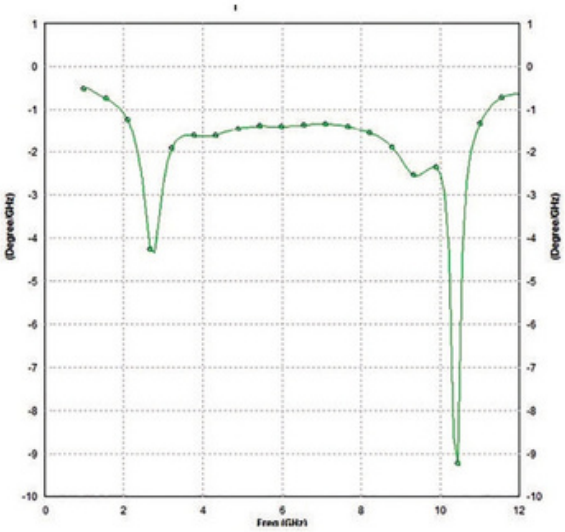

**Fig. 16: Simulation Results of Group Delay Vs. Operating Frequency of Design 3.**

The in-band return and insertion losses are good (i.e. $|S_{11}|$ ≥ -10 dB, and $|S_{21}|$ ≤ −1 dB) with frequency selectivity at both edges is high. The green line indicates the $S_{21}$ and other colour line indicates the $S_{11}$ as shown in Figure 15. Figure 16 shows group delay within whole UWB passband. A flat group delay. Coplanar waveguide structure is utilized to get multiple resonances and to make the band as flat as possible, quarter wavelength microstrip resonators are deployed. The simulation results shows good transmission characteristics, reflection characteristics and group delay within band of interest (Mentor Graphics Manual 2020). The transmission coefficient $S_{21}$ is given as (Hao et al.2010, Hong et al. 2001).

$$S_{21} = \frac{(Z_{even} - Z_{odd})Z_0}{(Z_{even} + Z_0)(Z_{odd} + Z_0)} \quad (9)$$

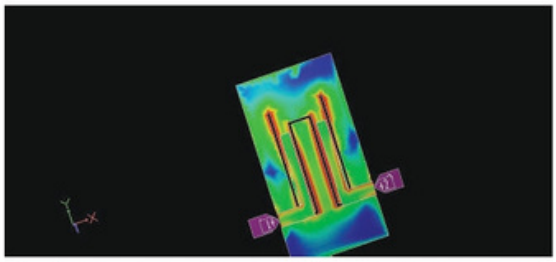

**Fig. 17: Simulation Results of Current Distribution Vs. Operating Frequency of Design 3.**

## CONCLUSION

The UWB technology will be the more popular for high speed wireless communication and it will provide key solution for the future wireless personal area network (WPAN) systems and is gaining momentum. A detail experimental work of UWB bandpass filter is presented in this study. Alongside, the design and analysis of three (design 1, design 2 and design 3) UWB BPF structures is carried out. The UWB bandpass filter of design 1 gives a return loss less than -20 dB, flat group delay, very less insertion loss at every frequency point within whole UWB. In design 1 The 10 dB bandwidth is from 3.29 GHz to 8.00 GHz. Thus the passband width is 4.71 GHz. The fractional bandwidth (FB) is 78.5%. In design 2 The 10 dB bandwidth starts from 2.99 GHz to 10.55 GHz. The width of passband is (10.55-2.99) = 7.56 GHz. The FBW is 111.69%. The filter structure in design 2 gives five transmission poles. In design 3 the BPF gives a FB of 90 percent at a center frequency of 5.4, as well as poles at 1.95 and 10.36. The proposed filter can find the application in 5G and 6G tranreceiver front end design technology to achieve ubiquitous communications. The proposed UWB BPF has improved return loss performance i.e. -20 dB at every frequency within UWB. The insertion loss due to filter is very less. The size of filter is compact and suitable for UWB applications where compactness is an important design constraint.

## REFERENCES


A. Kamma, J. Mukherjee (2017) Multiple band notch and Dual-Band filter using concentric and contiguous split ring resonators (CCSRR), Journal of Electromagnetic Waves and Applications, 31(1):57-71.

Abu Nasar Ghazali, Mohd Sazid, Srikanta Pal (2018) Dual band notched UWB-BPF based on hybrid microstrip-to-CPW transition AEU - International Journal of Electronics and Communications, Volume 86:55-62.

Abu NasarGhazali, MohdSazid, SrikantaPal (2017)A compact broadside coupled dual notched band UWB-BPF with extended stopband AEU - International Journal of Electronics and Communications 82:502-507.

D. M. Pozar (1998) Microwave Engineering 2nd ed. New York: Wiley.

Gholamreza Karimi, YeganehPourasad, AliLalbakhsh, HesamSiahkamari (2019) Design of a compact ultra-narrow band dual band filter for WiMAX applicationAEU - International Journal of Electronics and Communications 110:1-5.

H. El Omari El Bakali, H. Elftouh, A. Farkhsi, A. Zakriti, M. El Ouahabi (2020) Design of a Super Compact UWB Filter Based on Hybrid Technique with a Notch Band Using Open Circuited Stubs AEM Journal 9(3):39-46.

Hamza el Omari el Bakali (2019) Design of a Compact UWB BPF Using a Hybrid Structure and a Staircase-Shaped DGS International Journal of Microwave and Optical Technology 14(5):306-313.

Hamza El Omari El Bakalia, Hanae Elftouha , Abdelkrim Farkhsia , Alia Zakritib (2020) A Compact UWB Bandpass Filter with WLAN Band Rejection Using Hybrid Technique Elsevier B.V. 46:922-926.

He Zhu, Sai Wai Wong, Shenjie Wen, and Qing Xin Chu (2013) An Ultra-wideband (UWB) Bandpass Filter with Microstrip-to-CPW Transition and a Notch-band IEEE.

Hussain Bohra; Amrit Ghosh; Anand Bhaskar; Arvind Sharma (2020) A Miniaturized Notched Band Microstrip Wideband Filter with Hybrid Defected Ground Structure Technique published in Third IEEE International Conference on Smart Systems and Inventive Technology (ICSSIT) 745-750.

J. S. Hong and M. J. Lancaster (2001)Microstrip Filters for RF/ Microwave Applications New York: Wiley.

Jagadish B Jadhav and Pramod J Deore (2017) A compact planar ultra-wideband bandpass filter with multiple resonant and defected ground structure AEU - International Journal of Electronics and Communications 81:31-36.

Jagadish Baburao Jadhav, Pramod Jagan Deore (2017) Filtering antenna with radiation and filtering functions for wireless applications," Journal of Electrical Systems and Information Technology 4(1):125-134.

Jia-Kang Wu, Jun-Ge Liang, Xiao Wang, Nam-Young Kim, Xiaofeng Gu (2021) Multi-band bandpass filter based on direct-connected T-shaped stub-loaded resonator.

L. Wu, P. Hu, C. Li, L. Li, C. Tang (2019) A Novel Compact Microstrip UWB BPF with Quad Notched Bands Using Quad-Mode Stepped Impedance Resonator, Progress In Electromagnetics Research Letters 83:51–57.

M. Roberg and C. Campbell (2013) A Novel Even & Odd-Mode Symmetric Circuit Decomposition Method IEEE Compound Semiconductor Integrated Circuit Symposium (CSICS) 1-4.

Mentor Graphics HyperLynx IE3D electromagnetic simulator Manual 2020.

Mohd Sazid N.S.Raghava (2021) Planar UWB-bandpass filter with multiple passband transmission zeros AEU - International Journal of Electronics and Communications 134.

Rainee N. Simons (2001) Coplanar Waveguide Circuits, Components and Systems John Wiley & Sons, Inc.

S. C. Gupta, M. Kumar, R. S. Meena (2017)Design and Analysis of Triple Notched Band Uwb Band Pass Filter Using Defected Microstrip Structure (Dms), International Journal of Wireless Communications and Mobile Computing 5(6):32-44.

Tian-xiang Hu; Ying-hong Zhang; Xiao Wei; Zheng-hua Qian (2019) Design of an Ultra-Wideband Band-Passfilter Circuit for Electromagnetic Ultrasonic Signal Condition 13th Symposium on Piezoelectrcity, Acoustic Waves and Device Applications (SPAWDA).

Vikram Sekar and Kamran Entesari (2011) Miniaturized UWB Bandpass Filters With Notch Using Slow-Wave CPW Multiple-Mode Resonators IEEE Microw. Wireless Compon. Lett., 21 (2):80-82.

X. Guo, Y. Xu, W. Wang (2015) Miniaturized Planar Ultra-Wideband Bandpass Filter with Notched Band, Journal of Computer and Communications 3:100-105.

X. Liu, C. Zhong, H. Song, Y. Chen, T. Luo (2018) A New Compact Microstrip UWB Bandpass Filter with Triple-Notched Bands and Good Stopband Performance, Progress In Electromagnetics Research Letters 72:29–37.

X. Luo, J.-G. Ma, K. Ma, and K. S. Yeo (2010) Compact UWBbandpass filter with ultra narrow notched band IEEE Microw. Wireless Compon. Lett., 20 (3):145–147.

ZarkoSakotic, Vesna Crnojevic-Bengin Nikolina Jankovic(2017) Compact circular-patch-based bandpass filter for ultra-wideband wireless communication systems AEU - International Journal of Electronics and Communications 82.

Zhang-Cheng Hao and Jia-Sheng Hong (2010) Ultrawideband Filter Technologies IEEE Microw. Mag., 56-68.